SSC-243

(SL-7-3)

SSC 243

STRUCTURAL ANALYSIS OF SS-7 CONTAINERSHIP UNDER COMBINED LOADING OF VERTICAL, LATERAL AND TORSIONAL MOMENTS USING FINITE ELEMENT TECHNIQUES

SHIP STRUCTURE COMMITTEE

1974

SHIP STRUCTURE COMMITTEE

AN INTERAGENCY ADVISORY
COMMITTEE DEDICATED TO IMPROVING
THE STRUCTURE OF SHIPS

MEMBER AGENCIES:

UNITED STATES COAST GUARD
NAVAL SHIP SYSTEMS COMMAND
MILITARY SEALIFT COMMAND
MARITIME ADMINISTRATION
AMERICAN BUREAU OF SHIPPING

ADDRESS CORRESPONDENCE TO:

SECRETARY
SHIP STRUCTURE COMMITTEE
U.S. COAST GUARD HEADQUARTERS
WASHINGTON, D.C. 20590

SSC-243

8 AUG 1974

This report is one of a group of Ship Structure Committee Reports which describes the SL-7 Instrumentation Program. This program, a jointly funded undertaking of Sea-Land Service, Inc., the American Bureau of Shipping and the Ship Structure Committee, represents an excellent example of cooperation between private industry, regulatory authority and government. The goal of the program is to advance understanding of the performance of ships' hull structures and the effectiveness of the analytical and experimental methods used in their design. While the experiments and analyses of the program are keyed to the SL-7 Containership and a considerable body of data will be developed relating specifically to that ship, the conclusions of the program will be completely general, and thus applicable to any surface ship structure.

The program includes measurement of hull stresses, accelerations and environmental and operating data on the SS Sea-Land McLean, development and installation of a microwave radar wavemeter for measuring the seaway encountered by the vessel, a wave tank model study and a theoretical hydrodynamic analysis which relate to the wave induced loads, a structural model study and a finite element structural analysis which relate to the structural response, and installation of long term stress recorders on each of the eight vessels of the class. In addition, work is underway to develop the initial correlations of the results of the several program elements.

Results of each of the program elements will be published as Ship Structure Committee Reports and each of the reports relating to this program will be identified by an SL- designation along with the usual SSC- number. A list of all of the SL- reports published to date is included on the back cover of this report.

This report contains the finite element structural analyses of the vessel.

W. M. Benkert

W. M. Benkert
Rear Admiral, U. S. Coast Guard
Chairman, Ship Structure Committee

SSC-243

(SL-7-3)

STRUCTURAL ANALYSIS OF SL-7 CONTAINERSHIP UNDER COMBINED LOADING OF VERTICAL, LATERAL AND TORSIONAL MOMENTS USING FINITE ELEMENT TECHNIQUES

by

A. M. Elbatouti, D. Liu, and H. Y. Jan

American Bureau of Shipping

This document has been approved for public release and sale; its distribution is unlimited.

U. S. Coast Guard Headquarters
Washington, D.C.
1974

ABSTRACT

The entire SL-7 container vessel hull structure is analyzed by the DAISY finite element computer program. The ship, loaded with containers, placed in oblique quasi-static regular waves, is subject to combined vertical, lateral and torsional loads. Stress distributions particularly in the deck region are presented and investigated from the analysis using the reduced element substructure feature in the program. Fine mesh analyses are also presented at different locations of the ship. The computed stresses are discussed in connection with the placement of strain gages instrumentation on the "SEA-LAND McLEAN".

CONTENTS

LIST OF FIGURES

LIST OF FIGURES (Cont'd)

SHIP STRUCTURE COMMITTEE

The SHIP STRUCTURE COMMITTEE is constituted to prosecute a research program to improve the hull structures of ships by an extension of knowledge pertaining to design, materials and methods of fabrication.

RADM W. M. Benkert, USCG, Chairman
Chief, Office of Merchant Marine Safety
U.S. Coast Guard Headquarters

CAPT J. E. Rasmussen, USN
Head, Ship Systems Engineering
and Design Department
Naval Ship Engineering Center
Naval Ship Systems Command

Mr. M. Pitkin
Asst. Administrator for
Commercial Development
Maritime Administration

Mr. K. Morland
Vice President
American Bureau of Shipping

CAPT L. L. Jackson, USN
Maintenance and Repair Officer
Military Sealift Command

SHIP STRUCTURE SUBCOMMITTEE

The SHIP STRUCTURE SUBCOMMITTEE acts for the Ship Structure Committee on technical matters by providing technical coordination for the determination of goals and objectives of the program, and by evaluating and interpreting the results in terms of ship structural design, construction and operation.

NAVAL SHIP SYSTEMS COMMAND

Mr. P. M. Palermo - Member
Mr. J. B. O'Brien - Contract Administrator
Mr. G. Sorkin - Member
Mr. C. H. Pohler - Member

U.S. COAST GUARD

CDR C. S. Loosmore - Secretary
CAPT D. J. Linde - Member
CDR E. L. Jones - Member
CDR W. M. Devlin - Member

MARITIME ADMINISTRATION

Mr. J. J. Nachtsheim - Chairman
Mr. F. Dashnaw - Member
Mr. F. Seibold - Member
Mr. R. K. Kiss - Member

MILITARY SEALIFT COMMAND

Mr. R. R. Askren - Member
Mr. T. W. Chapman - Member
CDR A. McPherson, USN - Member
Mr. A. B. Stavovy - Member

AMERICAN BUREAU OF SHIPPING

Mr. S. G. Stiansen - Member
Mr. I. L. Stern - Member

NATIONAL ACADEMY OF SCIENCES
Ship Research Committee

Mr. R. W. Rumke - Liaison
Prof. J. E. Goldberg - Liaison

SOCIETY OF NAVAL ARCHITECTS & MARINE ENGINEERS

Mr. T. M. Buermann - Liaison

BRITISH NAVY STAFF

CDR P. C. Bryan, RCNC - Liaison

WELDING RESEARCH COUNCIL

Mr. K. H. Koopman - Liaison

INTERNATIONAL SHIP STRUCTURES CONGRESS

Prof. J. H. Evans - Liaison

U.S. COAST GUARD ACADEMY

CAPT C. R. Thompson - Liaison

U.S. MERCHANT MARINE ACADEMY

CAPT W. M. Maclean - Liaison

U.S. NAVAL ACADEMY

Dr. R. Bhattacharyya - Liaison

CHAPTER I

Introduction

The finite element analysis of the entire hull structure of the SL-7 container ship is an effort towards better understanding of the response of container ships in an oblique seaway.

With hatch openings approaching 85% of the ship's beam, the torsional rigidity of the container ship's hull girder is considerably different from that of the traditional cargo ship whose torsional rigidity was approximated by the assumption of a closed box hull girder cross section. Further, the abrupt changes in deck stiffness at the engine room housing and at the closed ends of the vessel may accentuate longitudinal stresses due to the warping restraint present at these locations. Numerous questions and speculations were raised concerning the stress level and/or deformations at various locations of the deck structure. Accordingly, the reduced element substructure technique is used in the finite element modelling of these areas of concern. (1), (3)*.

The reduced element substructure approach can briefly be described as a local analysis of a refined model within the overall analysis. An automatic process for reducing the interactive freedoms between the substructure and the rest of the structure using interpolation functions is employed. The more refined local model is integrated within the computation of the overall ship analysis and local results can be automatically generated. The procedure is comparable to finite element substructuring, with the exception that the desirable feature of interpolation of boundary displacements is automatically provided for. This feature is most useful in the transition region between a fine and coarse grid, wherein interpolation ensures displacement compatibility between adjacent elements. (3). Chapter II describes the ship modelling in further detail.

The general purpose finite element structural program DAISY (Displacement Automated Integrated SYstem) is the nucleus of the ship structural analysis package (4), (5). It calculates the nodal point deflections and element stresses of the idealized structure subject to the idealized loadings at the nodes.

The loadings and structural idealizations are carried out with the help of preprocessor programs listed below in the order of their use: (6).

---

* Numbers in brackets denote references at end of text.

Preprocessor Programs

1. SHIP MOMENT - with the vessel's lines, steel, fuel and cargo weight distributions, and wave profile specified, the program performs a static balance of the vessel to determine sinkage and trim. Vertical shear and bending moments are calculated, and for a vessel in oblique waves, inertia loads are introduced so that quasi-static values of lateral and torsional moments are obtained.

2. EXAM - generates the finite element structural model of the hull structure. Using few inputs with the SHIPMOM outputs of draft, trim and wave profile, EXAM also automatically calculates the hydrostatic pressures at node points in the model.

3. EXPLOT - provides a CALCOMP line plot of the model generated by EXAM. The plots are two-dimensional and indicate nodal points and freedom patterns, as well as the elements. Plots of any or all of the structural portions of the vessel can be made.

4. LOADER - takes the EXAM output and rearranges it in a manner suitable for the DAISY program. It calculates the statically consistent nodal point loads from the nodal pressures provided by EXAM. It also calculates the weight of the individual structural elements and translates them into nodal point loads.

Stress plotting is carried out by a postprocessor program called "STRPLOT". It generates CALCOMP plots of the DAISY calculated stresses, either as principal stresses or coordinate stresses.

CHAPTER II

LOADINGS AND STRUCTURAL MODELLING

Loading on the Vessel

Forces acting on the vessel consist of its own steel weight, inertia forces, fuel, cargo weight, and sea way loads. The steel and cargo weights are well defined. Steel weights are automatically calculated from the geometric properties of the structural elements used in the model. The fuel loads are distributed on the tank bottom nodes. The container weights are represented as concentrated point loads acting on the double bottom and cross deck members, at the container corner locations. Inertia loads are estimated from the mass distribution of the vessel, and are applied so as to place the vessel in dynamic equilibrium. The sea loads are computed from the program SHIPMOM for the ship poised statically on a wave. Although this static calculation is admittedly highly idealized, a comparison had been made of the longitudinal strength calculations for the vessel fully loaded by static and dynamic methods. For the latter, the strip theory calculations as described by Grim (2) are used for comparison. Using a half wave height of 1.01 $\lambda^{0.4}$ where λ is the wavelength in feet, and calculating the longitudinal bending moments for various wavelengths and headings, both methods of calculation indicated the same critical loading condition. The condition that the vessel is heading 60° to a wave of one-half the ship length (wave crest amidships) produced the critical loading, Figure 1. In general, the static values are usually on the high side. However, an equivalent static simulation which produces the same magnitudes of sea loadings, considering some of the dynamic effects, seems a proper approximation for the time being.

Although the number of loading conditions that can be handled by the DAISY program is virtually unlimited, only a selected number of conditions were used in the DAISY analysis in view of the time and manpower required to analyze the computed results of each. The number of load conditions for the SL-7 container ship was six. For all conditions, the vessel was considered to carry a full load of fuel and containers, and only the vessel's loading and wave configuration were varied. Among the conditions analyzed by the DAISY program were the head wave and still-water condition, as well as several cases with the vessel headed 60° to various waves.

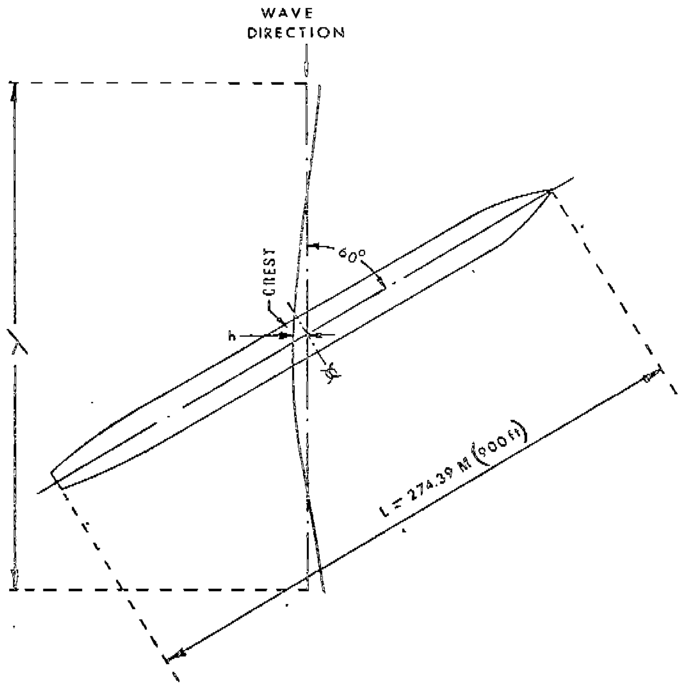

FIGURE 1 - WAVE GEOMETRY

	λ	h	λ/L
First loading case	246.95 m (810 ft)	8.972 m (29.43 ft)	0.9
Second loading case	192.073m (630 ft)	8.112 m (26.61 ft)	0.7

Two loading conditions yielded the highest deck stress values. The first loading case considers the vessel in a sinusoidal hogging wave of height 8.972 m (29.43 ft.) and a length of 246.95 m (810 ft.), λ/L =0.9, directed at 60 degrees from the ship's heading. This wave produced hull girder moment values equal to 75% of Grim's maximum vertical bending wave resultant value. The second loading case represented the vessel in a hogging wave of height 8.112 m (26.61 ft.) and a length of 192.073 m (630 ft.), λ/L = 0.7, directed at 60 degrees from the ship's heading. The wave-produced hull girder moment values are equal in magnitude to Grim's maximum vertical bending wave resultant value. Shear force and moment diagrams for these loadings are shown in Figures 2 and 3. Since the actual loadings applied on the finite element model are discrete, these curves do not represent the exact way the model is loaded but it would rather serve in visualizing the force and moment distribution along the ship and help in interpreting the computer results.

One difficulty that arises in this container ship analysis is that of the unsymmetrical sea loads on the vessel cross section due to an oblique wave. This necessitates the separation of the total loading into two components: one symmetric and the other anti-symmetric, provided that appropriate boundary conditions are applied at the vessel centerline plane. The symmetric and anti-symmetric components of the sea load are

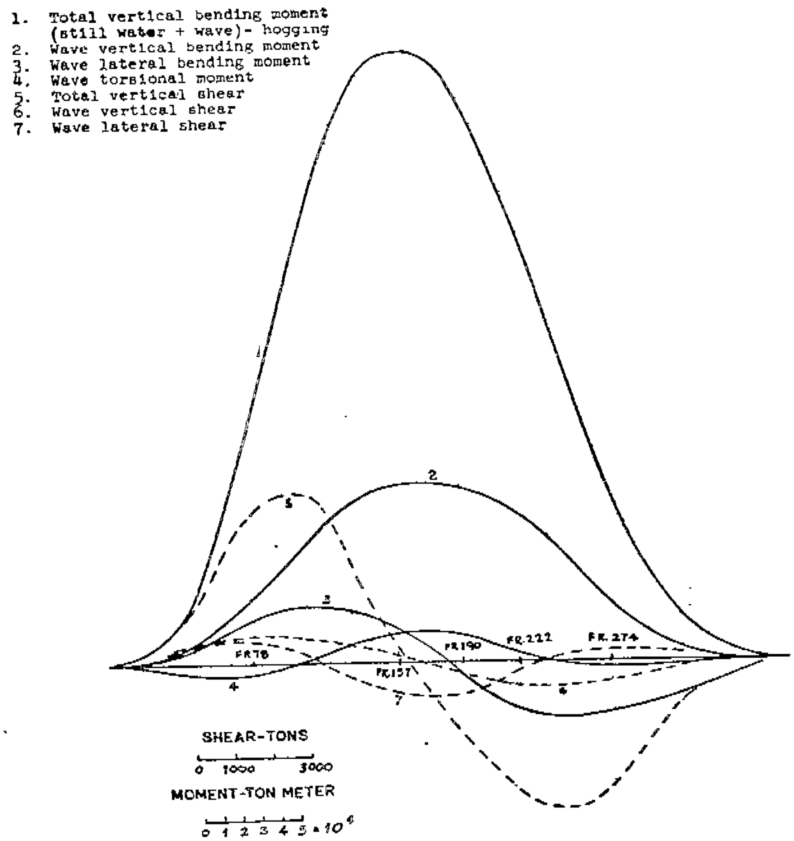

FIGURE 2 - FIRST LOADING CASE

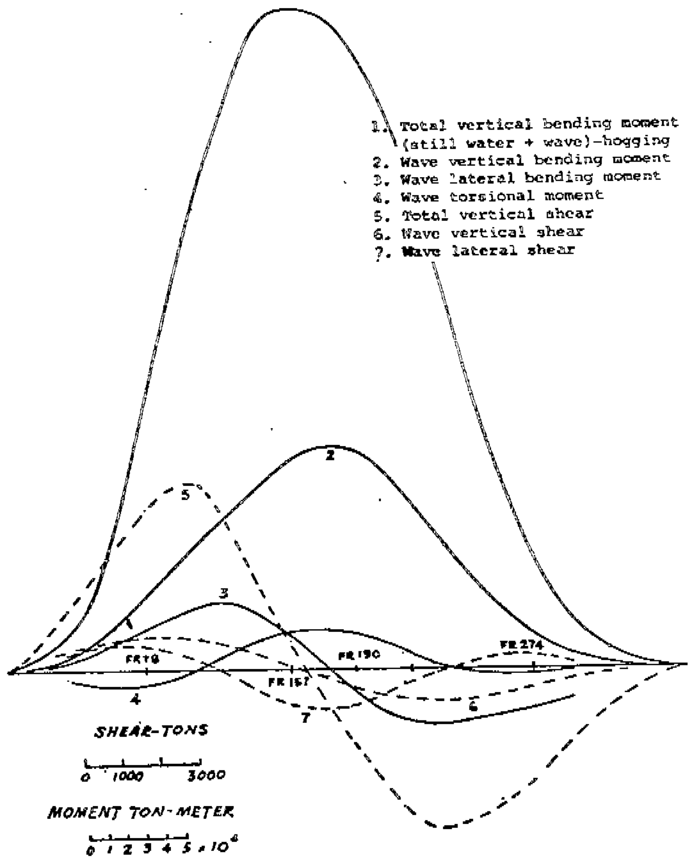

FIGURE 3 - SECOND LOADING CASE

illustrated on Figure 4. The symmetric components of the sea load would result in vertical shears and bending moments to be applied to the hull girder. The result of the anti-symmetric component is to cause only lateral and torsional bending of the hull girder. The partitioning of the total loading into the two components is automatically performed in the EXAM program. To obtain port and starboard side results, the DAISY program must be run twice with only one half of the ship modeled: once with symmetric loads and symmetric centerline nodal boundary freedoms and again with anti-symmetrical freedoms. The nodal displacements and element stresses must then be super-imposed accordingly to obtain port and starboard side results.

The use of symmetry and anti-symmetry is not necessary if both port and starboard sides of the vessel are modeled. However, to include both sides in the model increases the bandwidth of the master stiffness matrix and the number of unknown displacements by a factor of two and hence the computer solution time by a factor ranging between 6 and 8.

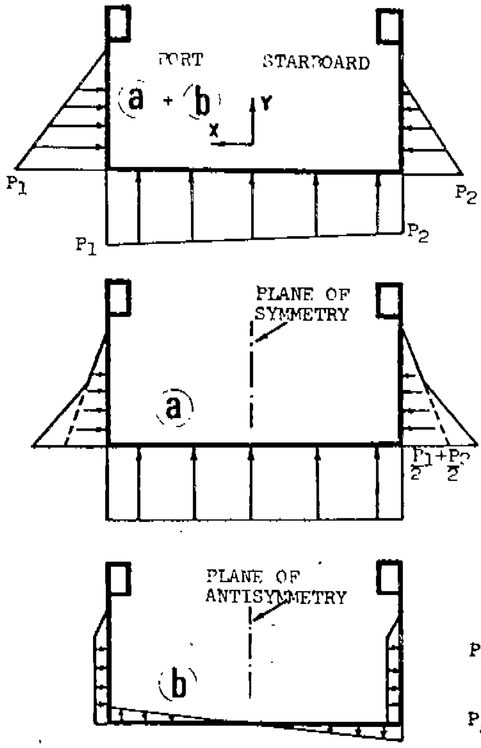

$$P_{sym}(x) = \frac{P(x) + P(-x)}{2}$$

$$P_{sym} = \frac{P_2 + P_1}{2}$$

$$P_{antisym}(x) = \frac{P(x) - P(-x)}{2}$$

$$P_{antisym} = \frac{P_1 - P_2}{2}$$

$$P_{stbd} = P_{symmetry} - P_{antisymmetry}$$

$$P_{port} = P_{symmetry} + P_{antisymmetry}$$

USE OF SYMMETRY AND ANTI-SYMMETRY
FIGURE 4 - LOADS ON THE SHIP

STRUCTURAL MODELLING

In order to fully represent the structural response of the hull girder to a torsional loading such as that due to the action of an oblique wave, it is necessary to model the complete 3-dimensional hull girder from bow to stern. Figures 5 and 6 show the general arrangements and a typical section of the containership.

To perform the analysis of the primary structure, one half of the entire hull, with the longitudinal centerline plane being the plane of structural symmetry, is idealized as a three dimensional finite element model using a variable size mesh. In the processoof automatic generation of the elements, the triangular flat plate elements are generated so that their plane surfaces are oriented to best fit the actual plate curvature. As an illustration to the coarse mesh generation, Figure 7 shows some of the generated elements in the shell, deck bottom and other major structural parts. (It is not intended to show the nodal numbers and the element symbols in such reduced scale).

Based on proposed strain gauge locations, different substructure models were employed at 23 different areas per one-half of the structure as shown in Figure 8. All the substructures are located in the deck mainly because the container vessel deck is subjected to higher deformations and stresses than other regions of the structure.

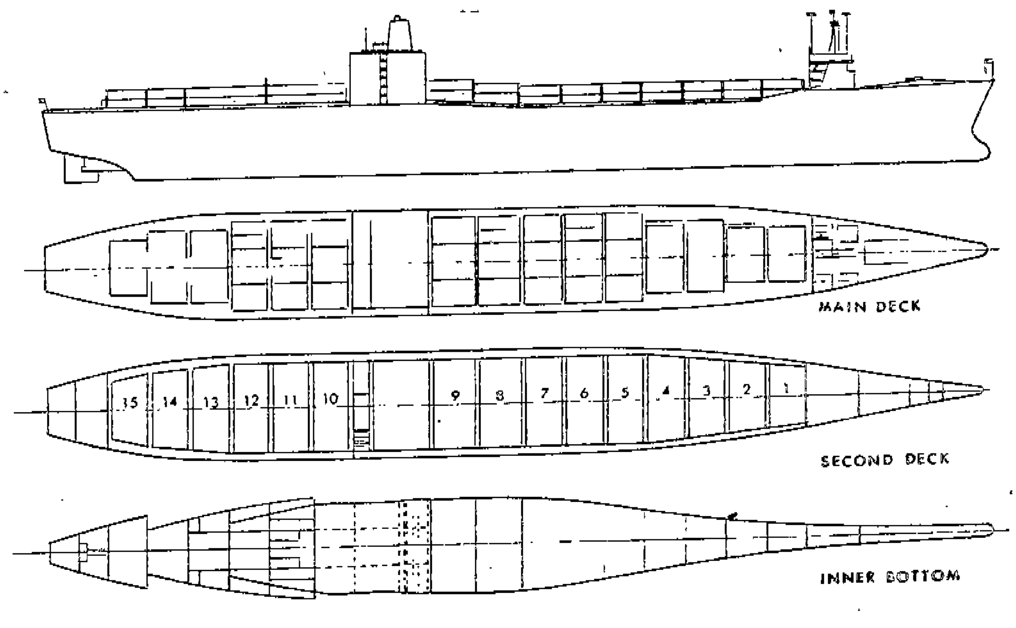

FIGURE 5 - SL-7 GENERAL ARRANGEMENT

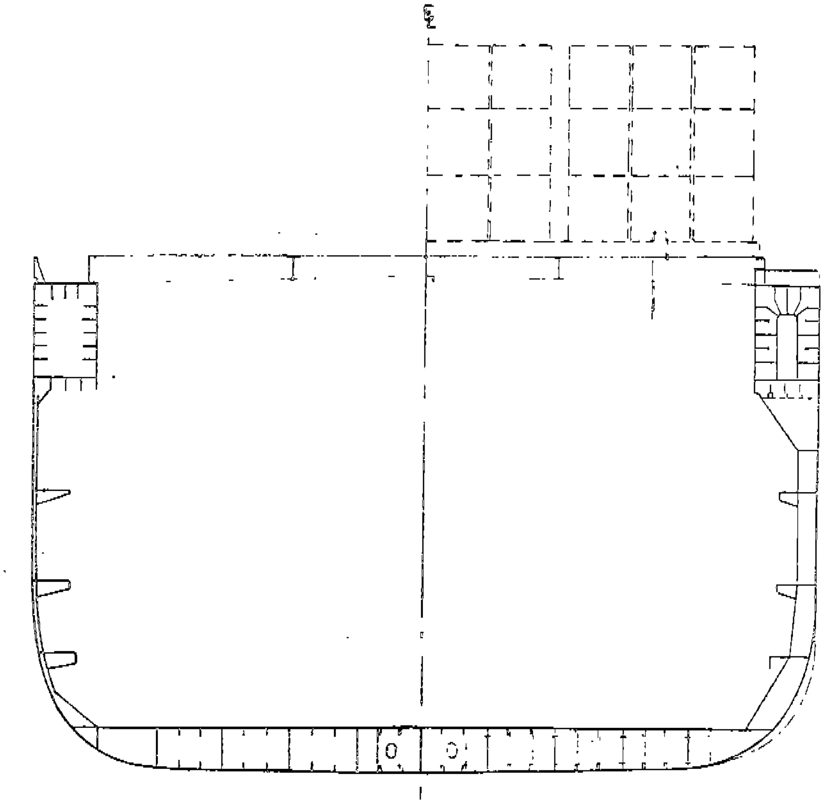

FIGURE 6 - SL-7 TYPICAL SECTION

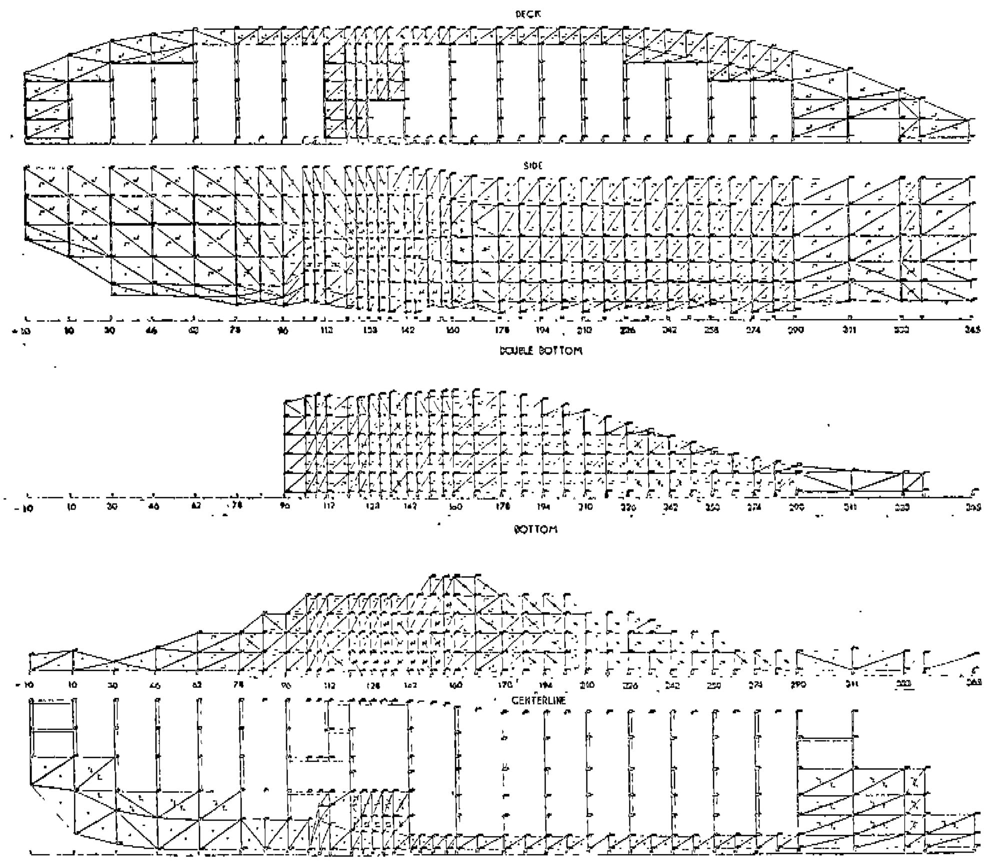

FIGURE 7 - COARSE MESH BEFORE SUBSTRUCTURING USING EXPLOT PROGRAM

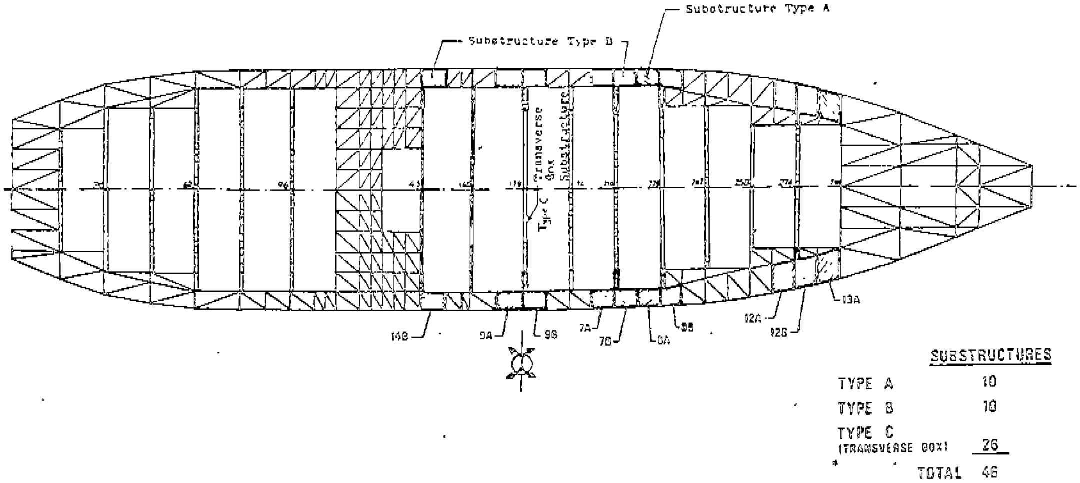

FIGURE 8 - SUBSTRUCTURE LAYOUT

Three substructure modules form the basic configuration for all substructures employed in the ship model. One module contains a portion of the side wing box; another module contains a part of the transverse box between hatches, and the third module contains parts of the side wing box and transverse wing box at hatch corner, Figure 9.

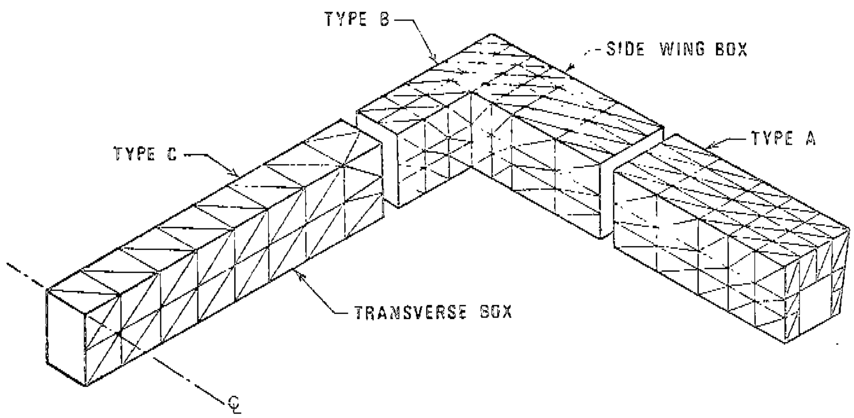

FIGURE 9 - SUBSTRUCTURE MODULES

The philosophy behind the use of the reduced element substructure technique is to eliminate the need for fine grids, remodelling of specific portions of the structure, and their costly computer reruns. The ideal use of this technique would be in a ship with repetitive forms of substructures in such a way that the grid modelling of one is usable for the others with minimum changes in some element characteristics or dimensions. This is not the case in SL-7 container ship. Because of the fineness of the hull structure, it was necessary to have twelve different substructure models. With such large numbers of substructures of variable dimensions and forms, it was uneconomical to use a very fine grid to represent all structural details.

The chosen mesh is believed to give a fair indication as to the stress level in the substructure. Also it would be enough to represent the true stiffness of its major structural members. The reduced element substructure which indicates high stress levels has been remodeled with very fine grids in order to obtain detailed stress distributions. Here all structural members are considered in the fine grid models. The table on page 11 provides more information about the problem size and the type of elements employed in the analyses.

BOUNDARY SUPPORTS

The ship is supported at three points as shown. The supports are essential to prevent rigid body movement.

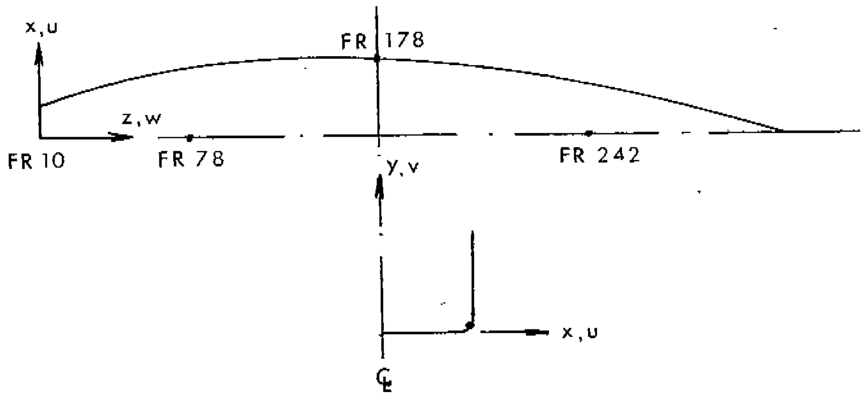

Ship frame number	78	178	242
Symmetrical loading	v = 0	w = 0	v = 0
Anti-symmetrical loading	u = 0	v = 0	u = 0

TABLE OF SL-7 FINITE ELEMENT MODELS

FINITE ELEMENT MODELS	TYPE OF FINITE ELEMENTS USED	NUMBER OF ELEMENTS	NUMBER OF UNKNOWNS
A. WHOLE STRUCTURAL MODEL (Fig. 7) One-half ship model including all master nodes of the reduced element substructure.	Eccentric beams, orthotropic triangular bending elements, isotropic triangular bending elements and bars.	4570	5233
SUBSTRUCTURE: (Figs. 8, 9, 10)			
Transverse box girder, Frame 2	Isotropic triangular bending elements and bars.	102	268
Transverse box girder, Frames 4, 5, 6, 8, 17, 21, 23, 25, 27, 29, 31, each	"	140	338
Substructure 14B	"	386	908
9A	"	263	631
9B	"	386	904
7A	"	263	630
7B	"	384	899
8A	"	242	584
8B	"	372	889
12A	"	319	742
12B	"	329	791
13A	"	218	536
B. FINE MESH MODELS (Figs. 11, 12)			
MODEL 1 Frames 176 to 182	Membrane quadrilateral and triangular elements and eccentric beams	976	1617
MODEL 2 Frames 142 to 146	Membrane quadrilateral and triangular elements, eccentric beams and isotropic triangular bending elements	805	1663
MODEL 3 Frames 151 to 160	Membrane quadrilateral elements and eccentric beams	204	339
MODEL 4 Frames 186 to 194	Membrane quadrilateral elements and eccentric beams	204	339

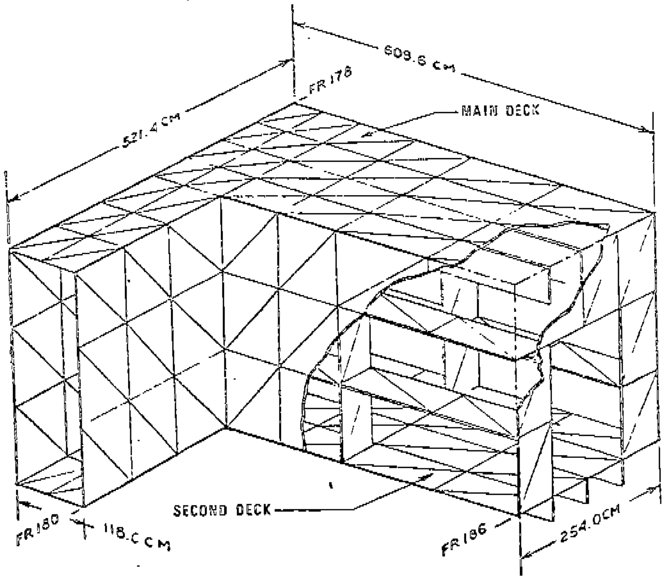

FIGURE 10 - GRID FORM OF SUBSTRUCTURE 9B AS AN EXAMPLE OF SUB. MESH SIZE

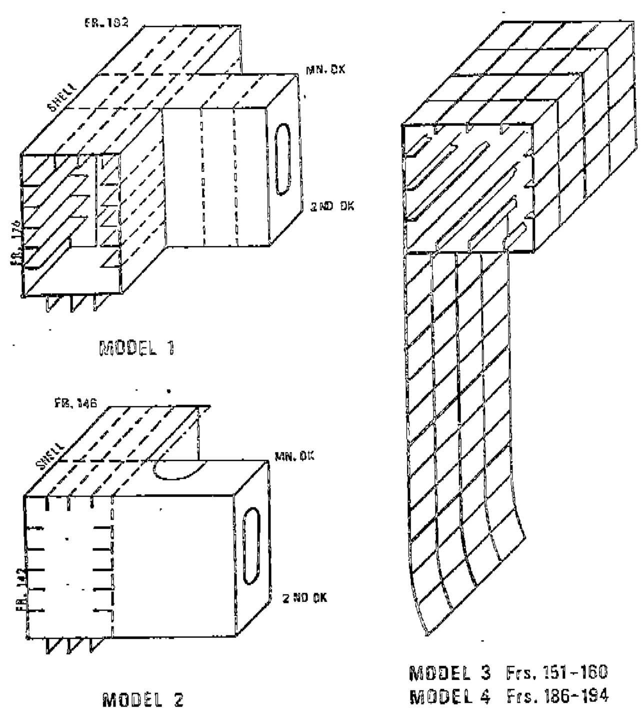

FIGURE 11 - FINE MESH MODELS OUTLINE

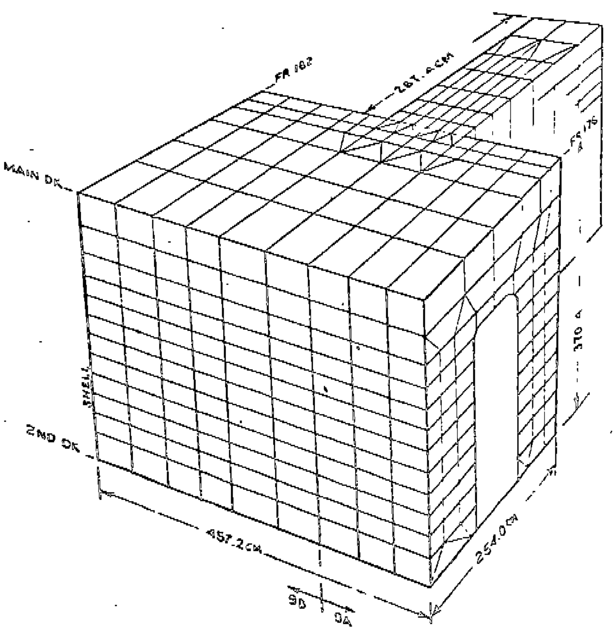

FIGURE 12 - GRID FORM FOR MODEL 1 AS AN EXAMPLE OF FINE MESH SIZE

CHAPTER III

RESULTS AND DISCUSSION

DISPLACEMENTS

Figure 13 illustrates the overall displacements of the deck for the first loading case.

The top view shows the vertical and longitudinal displacement components of the container ship main deck centerline, also the longitudinal displacement of the ship's side lines at selective frames, namely, ship frames 46, 160, 186 and 282. In the first curve, the vertical component of the displacement is due to pure longitudinal vertical bending of the ship hull girder. The longitudinal component is due to both vertical and torsional deformation of the hull. The second group of curves shows the resultant displacement due to torsional warping and lateral bending deformation of both deck side lines of the ship. It is clear that the longitudinal displacement of both sides are almost negligible, near midship.

The bottom view shows the displacements for the upper deck at the centerline and the ship's sides. The distortion of hatch diagonals has been calculated, and the initial diagonal lengths for the idealized structure are tabulated. For the first loading case, the maximum distortion is found to be at the second hatch opening forward of the engine room. The deformation gradually decreases towards the forward hatch.

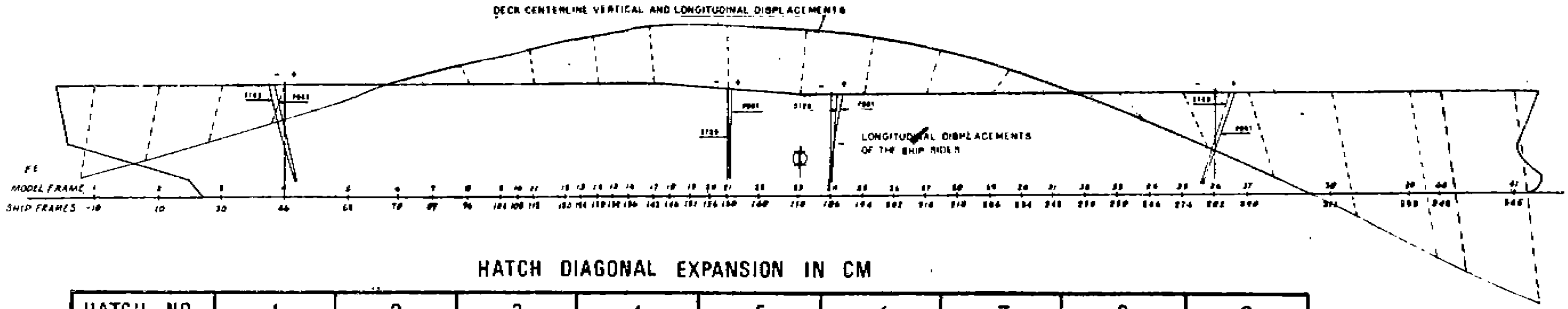

HATCH DIAGONAL EXPANSION IN CM

HATCH NO.	1	2	3	4	5	6	7	8	9
d	2048.197	2046.749	2494.283	2494.189	2969.781	2969.800	2965.790	3036.431	3036.469
EXPANSION	0.382	0.634	0.896	.125	1.510	2.056	1.989	2.413	1.695

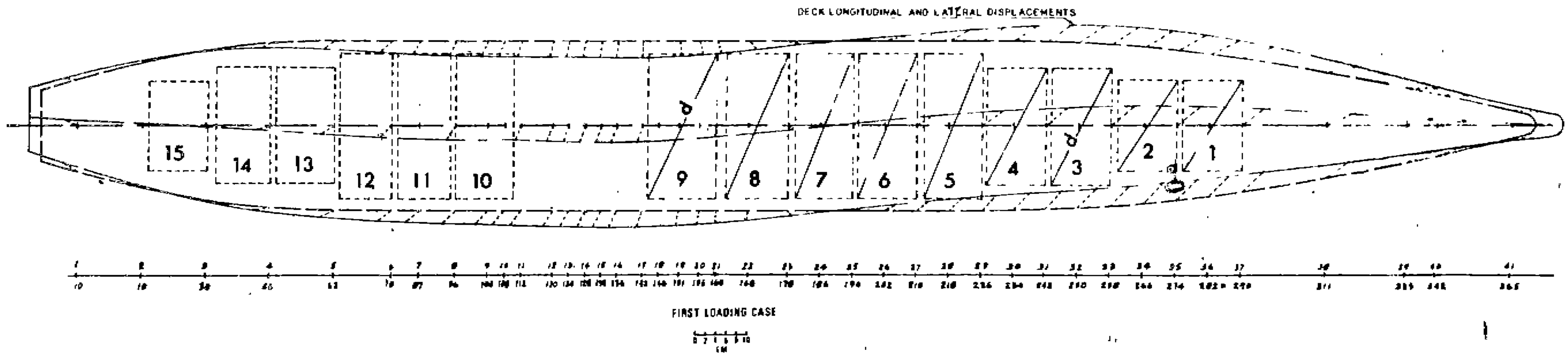

FIGURE 13 - OVERALL DISPLACEMENTS OF SL-7 DECK AND FRONT HATCHES DIAGONAL EXPANSIONS

Figure 14 shows the local deformation of the transverse box girders at ship frame 160. It shows the total deformation of the transverse box substructure at frame 160 and the decomposed deformation of the edge AA to symmetric and anti-symmetric components. The deflected shape is plotted relative to a midpoint on the box top. This allows us to visualize the substructure end distortions and the symmetric deformation due to shear lag in the transverse box.

Figure 15 shows an exaggerated view of the transverse box frame 178 with the hatch cover. Because of the scale difference, the angular deformation does not represent the true values. As expected, the S shaped distortion is clear.

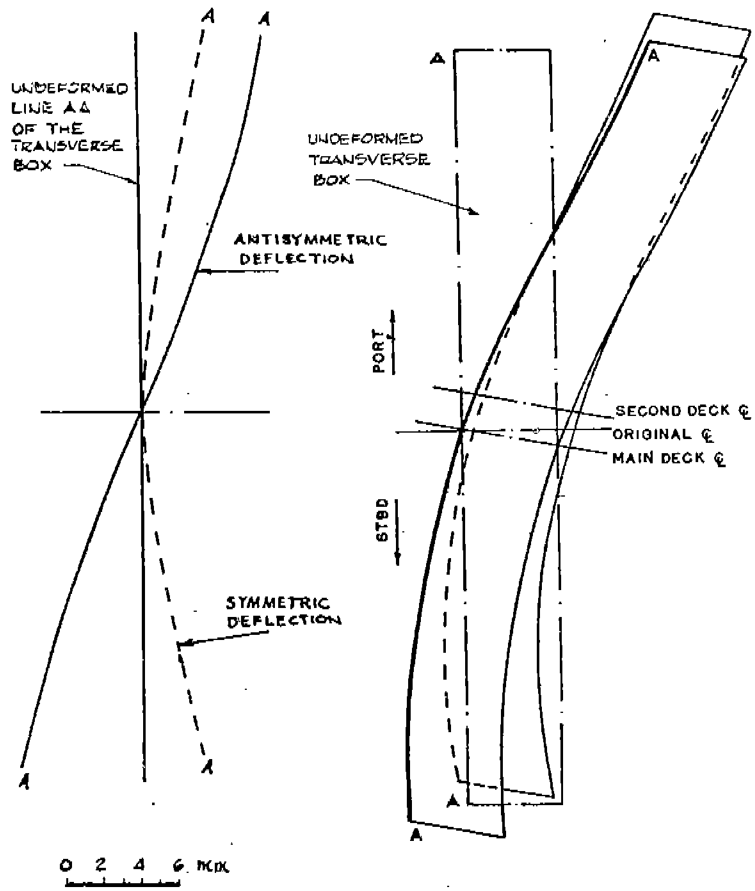

FIGURE 14 - DEFORMATION OF TRANSVERSE BOX Fr. 160 - First Loading Case

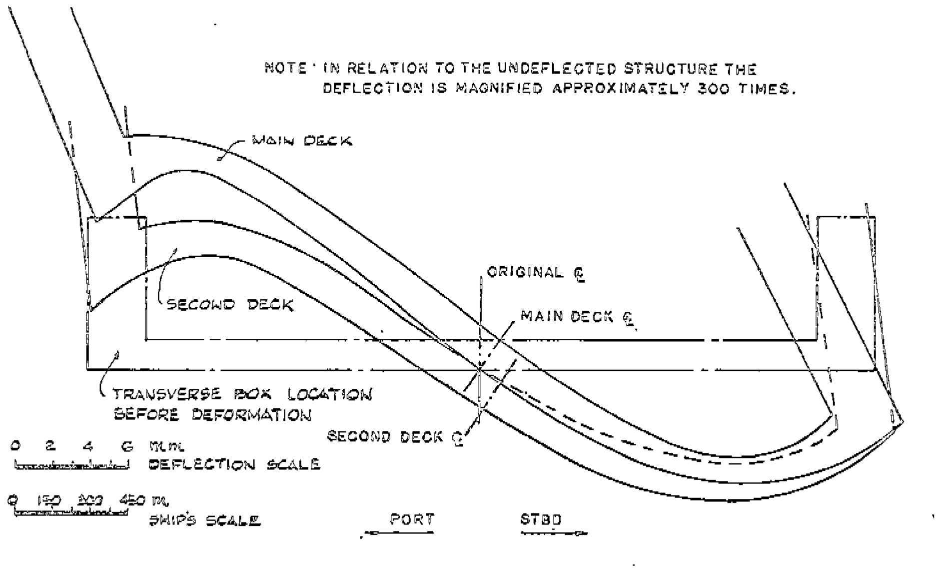

FIGURE 15 - DEFORMATION OF TRANSVERSE BOX Fr. 178 - First Loading Case

STRESSES

In running such extensive analyses by the finite element method, immense quantities of stresses are produced. The stresses at selective locations of the ship are examined and some of these locations coincide with the location of the strain gages installed on the container ship for full scale measurement. The other locations are chosen for reasoning the analysis. The interpretation of the computer results are focused on the first loading case. The second loading case is chosen whenever its results would better serve the purpose of the analysis.

Verification of the stress results creates a problem since there is no similar analysis or existing measurements presently available for comparison for this ship. The only option left is to analyze the computer results in light of the understanding of the structure's general response under simple forms of loadings. In this case the computed total stresses have to be resolved to the stress component pertinent to each type of loading, namely, vertical bending, lateral bending and twisting loads. The stress distribution of each resolved component is compared to its corresponding predicted stress form. This comparison, however, cannot verify the computed stress magnitudes. After the full-scale measurements will be available, further analyses and direct comparisons of the stress results are then feasible.

The combined stresses represented by the computer results can be resolved into its components by the following procedure:

pure longitudinal bending stress (due to symmetrical loadings only) = 1/2 (element stress results in specific direction port side + element stress results in the same direction starboard side).

The remaining anti-symmetric stresses includes both warping and lateral stresses.

In order to separate the warping stress from lateral stresses, lateral stresses are obtained simply by dividing the lateral bending moment value from the loading curve by the corresponding modulus section assuming the stress distribution as predicted by the elementary beam theory, Figure 16. This assumption is verified by the results shown in Figure 20.

Where triangular elements are used, the stresses were averaged for each two adjacent triangles. Curves are fitted when possible to help in visualizing the stress distribution.

General Ship Response to Combined Longitudinal, Lateral and Torsional Moments.

As previously discussed, the non-symmetric loads on the ship's sides are broken into symmetric and anti-symmetric components about the ship's centerline. This makes it possible to analyze one half of the ship. Accordingly, the total stresses are a superposition of the symmetric and anti-symmetric components as shown in Figure 16.

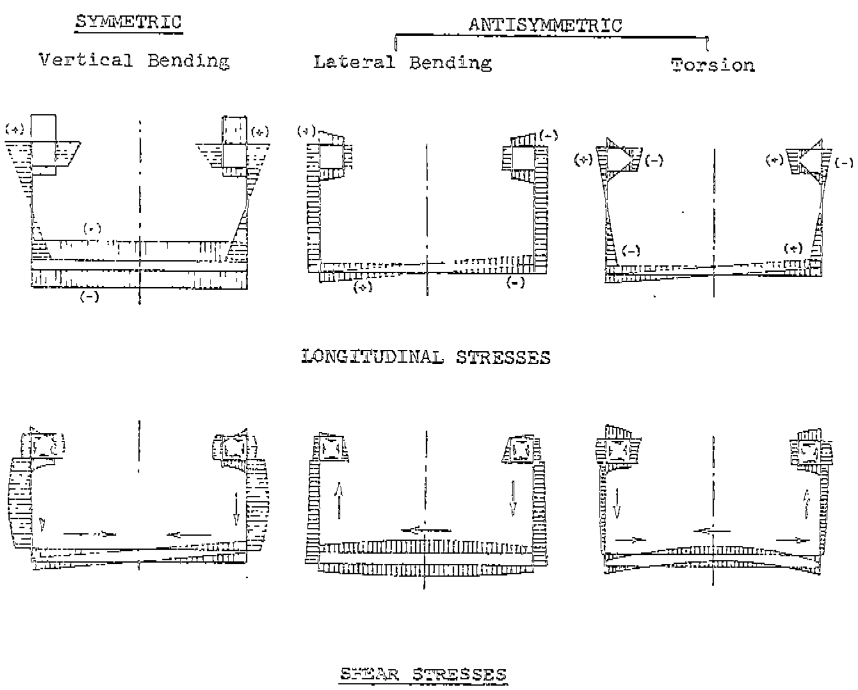

FIGURE 16 - PREDICTED DISTRIBUTION OF SYMMETRIC AND ANTI-SYMMETRIC STRESS COMPONENTS

Figure 16 shows predicted stress distributions based upon general structural response of a simple prismatic hull girder. Although we do not expect to have exact similar response from the finite element structural model, the stress distribution should generally have the same trend as those predicted above. Exceptions could be made for the stress distributions around the side wing boxes since the predicted stress distributions do not include many structural members as used in the substructure analysis.

SUBSTRUCTURE GENERAL RESPONSE

Within the three types of substructures described before, (Figures 8, 9), types A and B contain high stress values. To reason the stress form around the substructure wing box, the elementary beam theory is used neglecting stresses due to local effects. The longitudinal stress distribution then takes the form as shown in Figure 17.

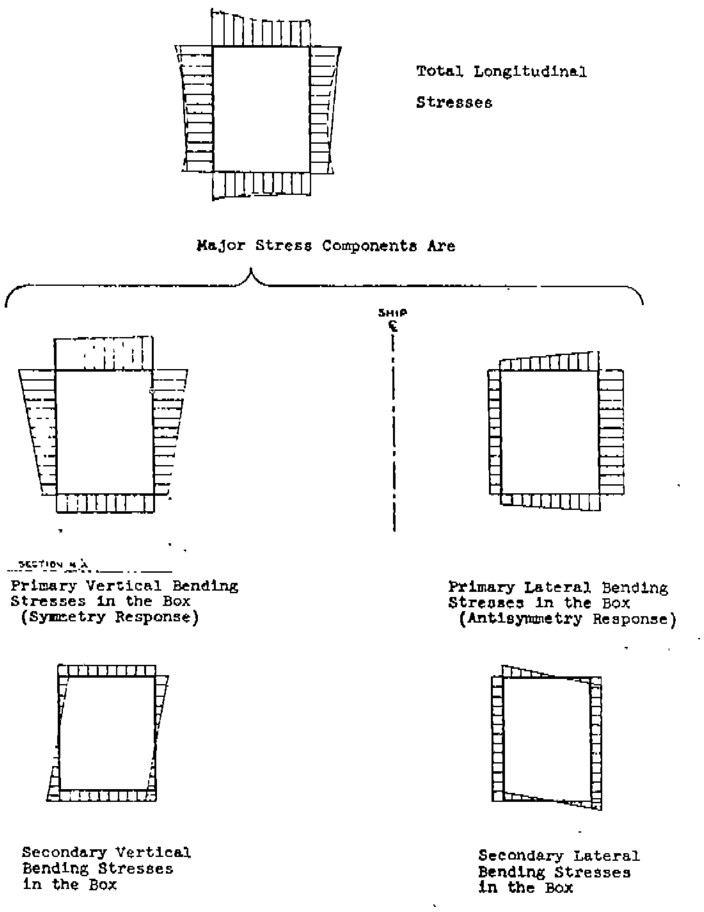

FIGURE 17 - WING BOX RESPONSES DUE TO BENDING MOMENT COMPONENTS

Due to local effects, the actual stress distribution will not be linear. The box corner rigidity provides restraint at the edges of each of the four plate panels. This will cause a little rise in stress values near box corners, and the actual distribution will be nonlinear as shown by the dotted line in Figure 17.

Different stress components are presented at various locations of the ship as designated by ship frame numbers,

<u>Section Frame 222</u> Figures 18 through 23

Section Frame 222 lies in an area of high vertical and lateral bending moments but the torsional moment is very small. The stresses of the deck side boxes are obtained from the result of substructure 8A. Side shell and bottom plating results are obtained from the coarse mesh analysis.

The longitudinal stresses due to combined loading is plotted for both port and starboard sides of the ship, Figure 18, in order to compare the stress components with those predicted before. The stresses due to pure vertical bending loads (symmetric loading case), and those due to combined lateral and torsional loads (anti-symmetrical loading case), are plotted in Figures 19 and 20 respectively. The finite element results on Figure 19 are confirmed by elementary beam theory calculations by using the bending moment value from Figure 2 and the calculated section modulus at Frame 222. Discrepancies are noticed in the results of the double bottom. In the finite element model the cargo and fuel loads are directly applied on the double bottom. The secondary stresses, defined as the stresses due to local hold loadings, are not accounted for in beam calculation and is believed to be a major cause of such discrepancies.

Figures 21, 22 and 23 represent the corresponding shear stress values for the total symmetric and anti-symmetric longitudinal loadings, respectively, for the first loading case. The anti-symmetric shear component, Figure 23, is very small relative to the shear induced by longitudinal vertical bending of the ship.

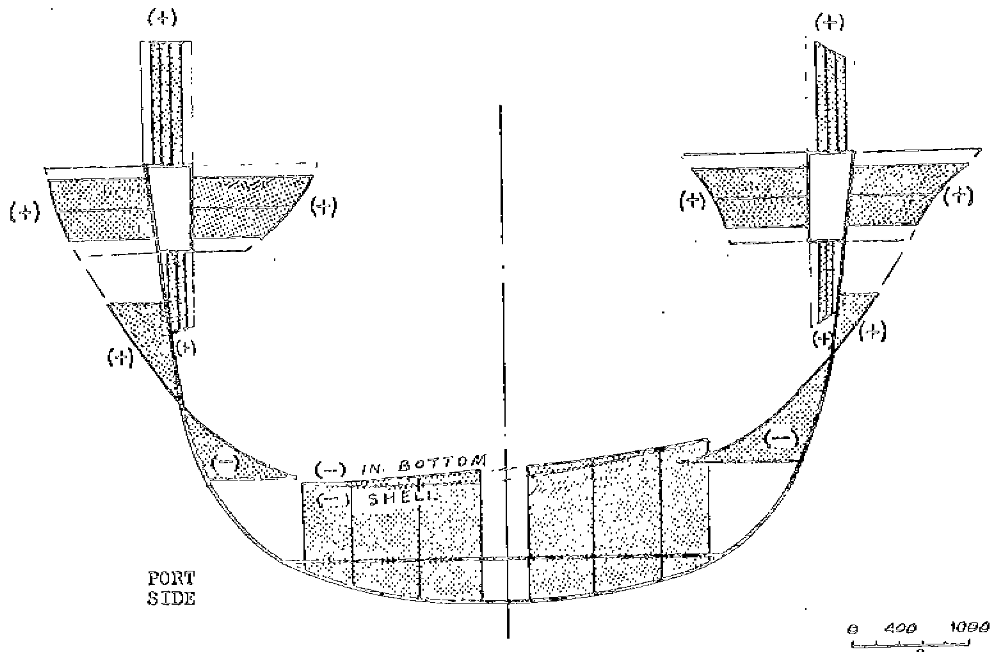

FIGURE 18 - TOTAL LONGITUDINAL STRESSES OF SECTION FRAME 222 (FIRST LOADING CASE)

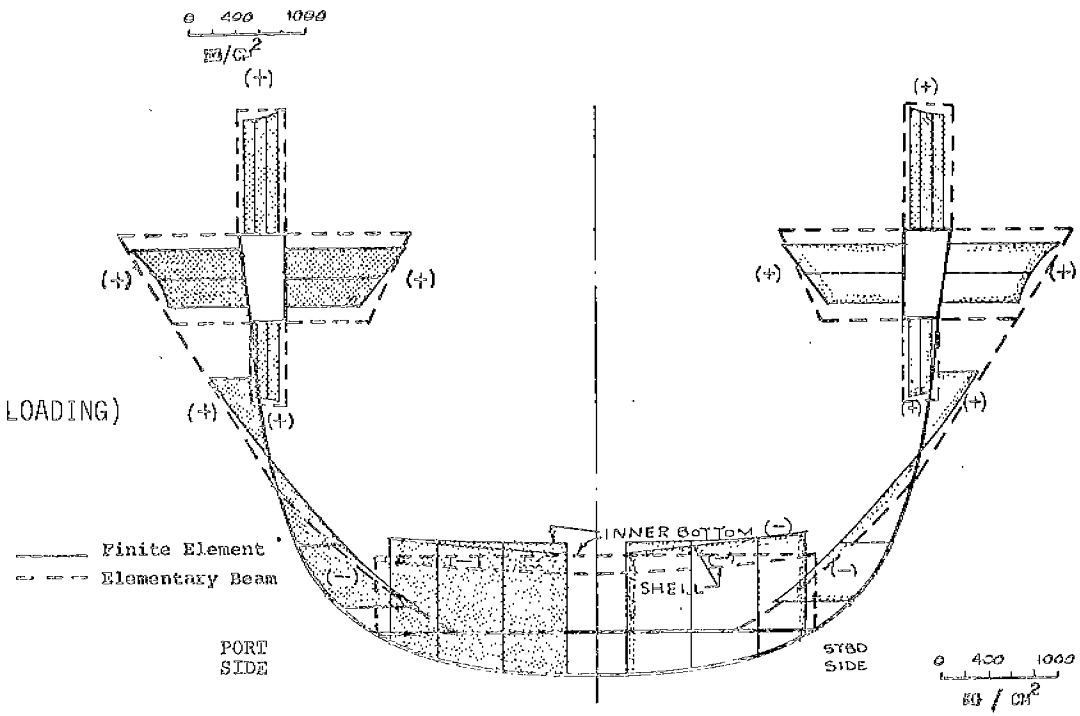

FIGURE 19 - LONGITUDINAL STRESSES DUE TO PURE VERTICAL BENDING LOADS OF SECTION FRAME 222 - (SYMMETRIC LOADING) (FIRST LOADING CASE)

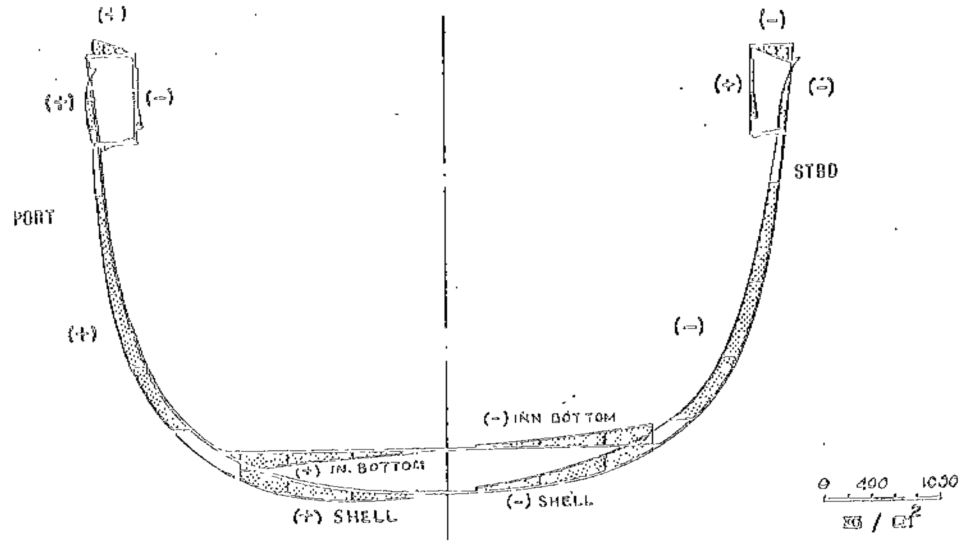

FIGURE 20 - LONGITUDINAL STRESSES DUE TO ANTI-SYMMETRICAL LOADINGS OF SECTION FRAME 222 (MAINLY DUE TO LATERAL BENDING LOADS)
(FIRST LOADING CASE)

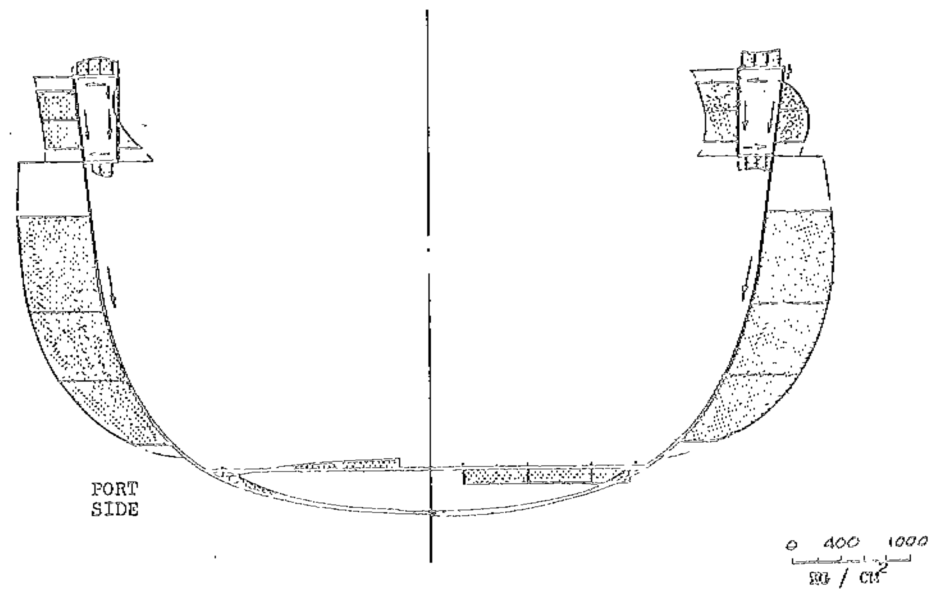

FIGURE 21 - TOTAL SHEAR STRESSES OF SECTION FRAME 222
(FIRST LOADING CASE)

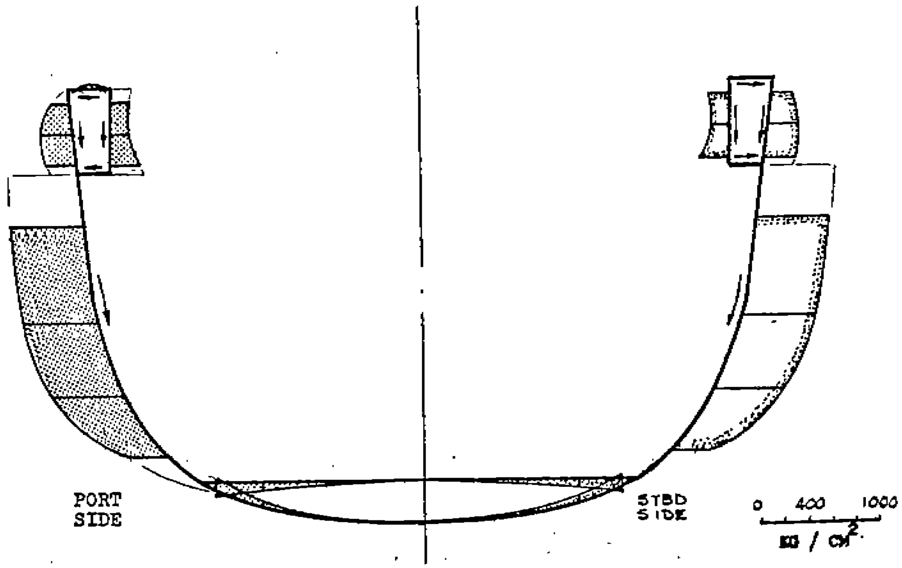

FIGURE 22 - SHEAR STRESSES DUE TO VERTICAL BENDING LOADS OF SECTION FRAME 222
(SYMMETRIC LOADING)
(FIRST LOADING CASE)

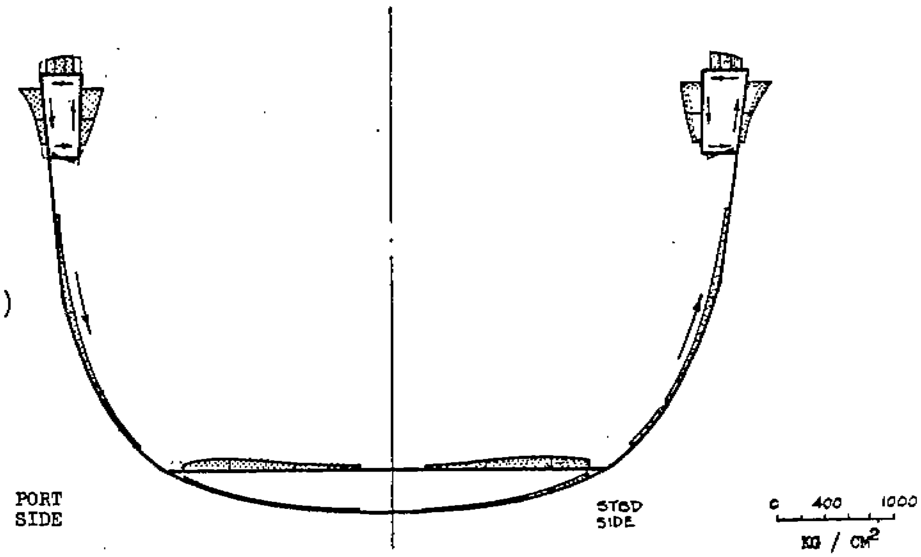

FIGURE 23 - SHEAR STRESSES DUE TO ANTISYMMETRICAL LOADINGS OF SECTION FRAME 222
(MAINLY DUE TO LATERAL BENDING LOADS)
(FIRST LOADING CASE)

Section Frames 156-158. Figures 24, 25.

This section is subjected to high values of combined moments for the second loading case. The presented stresses are taken from fine mesh analysis of Model 3 (Fig. 11). They correspond to the anti-symmetric component of the loadings. The stresses are resolved into two components corresponding to lateral bending (Figure 24) and torsion (Figure 25) respectively. For pure lateral bending (lateral shearing forces included), the stress components are obtained by utilizing the elementary beam theory. For pure torsion, the total computed values of warping and shear stresses for anti-symmetric loadings, less those shown in Figure 24, are plotted in Figure 25. It is worth noting that the distribution of torsional moment, as shown on the top of Figure 25, is arbitrarily referred to the base line of the vessel. This does not represent the true torsional moment on this section of the ship, but it serves the purpose of demonstrating the procedure of interpretation of the stresses without tackling the question of the exact location of the shear center for this type of vessel.

Section Frames 188-192. Figure 26.

The presented stresses here are taken from the fine mesh analysis of Model 4 (Fig. 11) running between frames 186 and 194. The computed longitudinal and shear stresses in the deck and side shell platings between Fr. 188-192 due to wave induced vertical moment and shearing force are plotted in Figure 26. The top diagram shows the distribution of loadings along the length of the vessel. It is interesting to note that the longitudinal stresses computed by means of both the finite element techniques and the elementary beam theory are in good agreement. This seems to confirm the validity of the beam approach for calculating the hull girder bending stresses for this type of vessel. The agreement is less for the shear stress distributions, which may be attributed to local bending not counted for in the beam approach.

Deck Wing Box Forward to Engine Room Housing Frames 142-150, Figures 27 through 31.

In the overall analysis of the ship, this part of the structure is modelled as substructure 14B. In the subsequent fine mesh analysis the portion from frames 142 to 146 is remodelled as shown in Fig. 11 as Model 2.

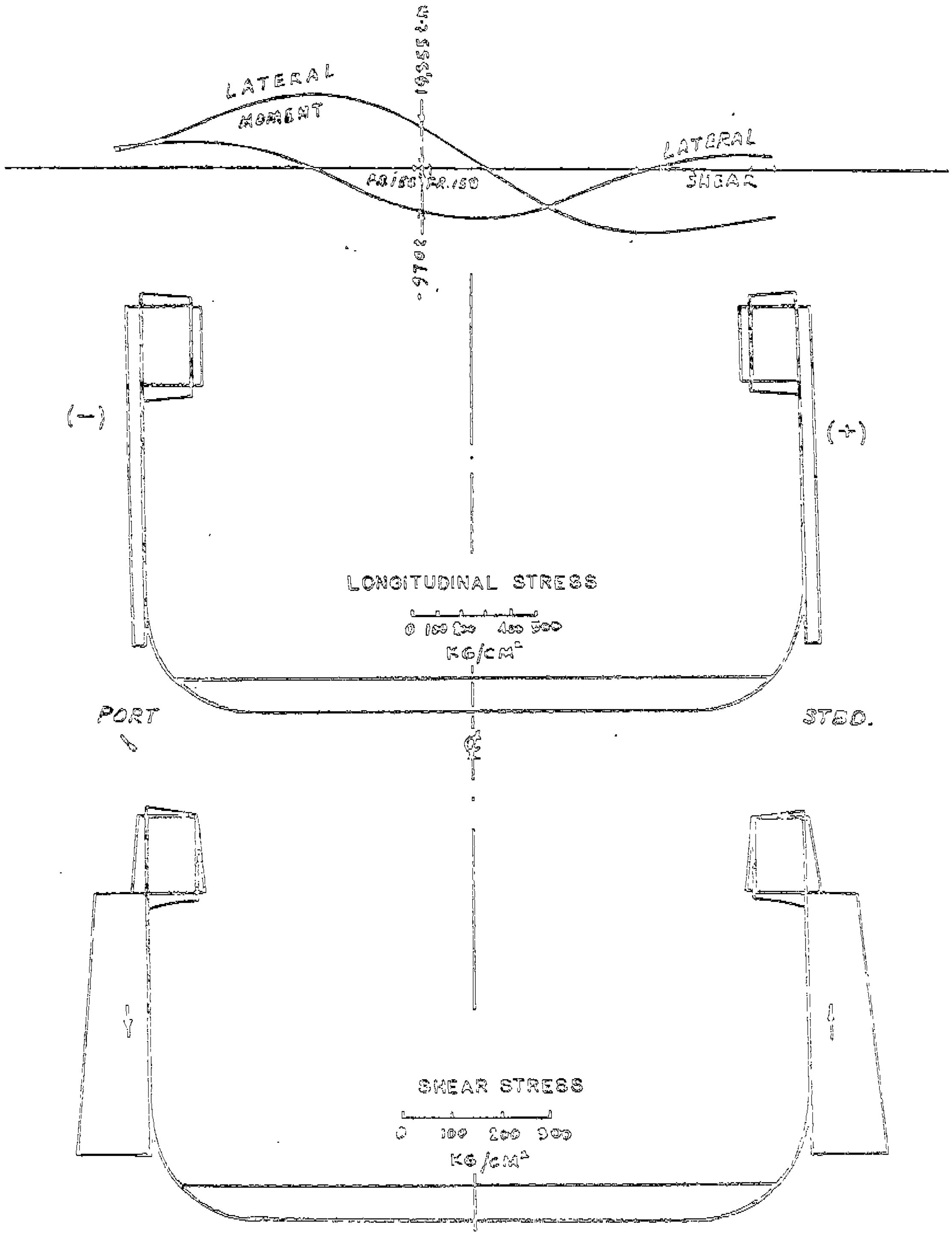

FIGURE 24 - STRESS DISTRIBUTIONS DUE TO LATERAL BENDING AND SHEAR FORCES AT FR 157 1/2 AS PREDICTED BY BEAM THEORY - SECOND LOADING CASE

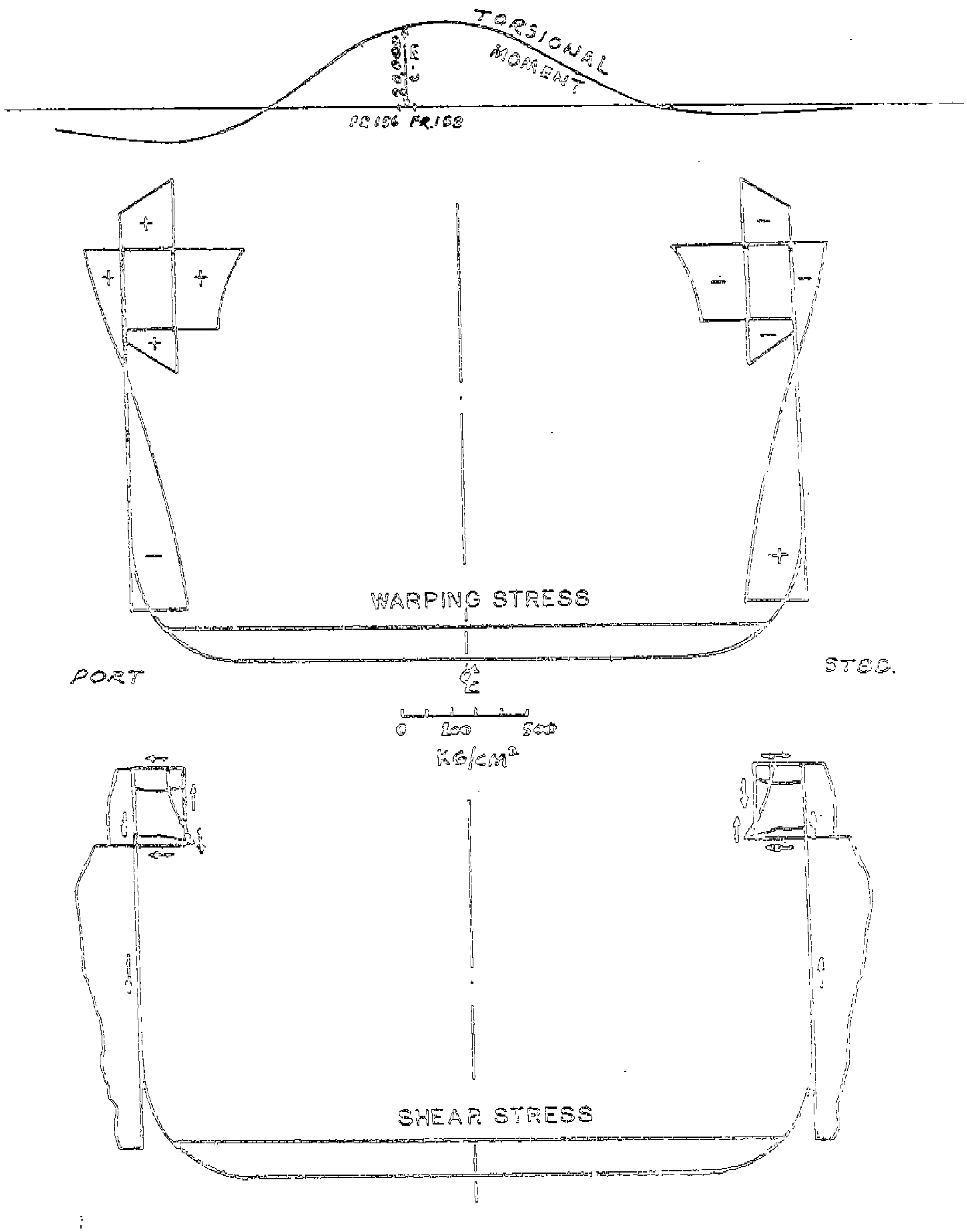

FIGURE 25 - STRESS DISTRIBUTIONS DUE TO TORSION AT FR 157 1/2
AS CALCULATED BY F. E. METHOD - SECOND LOADING CASE

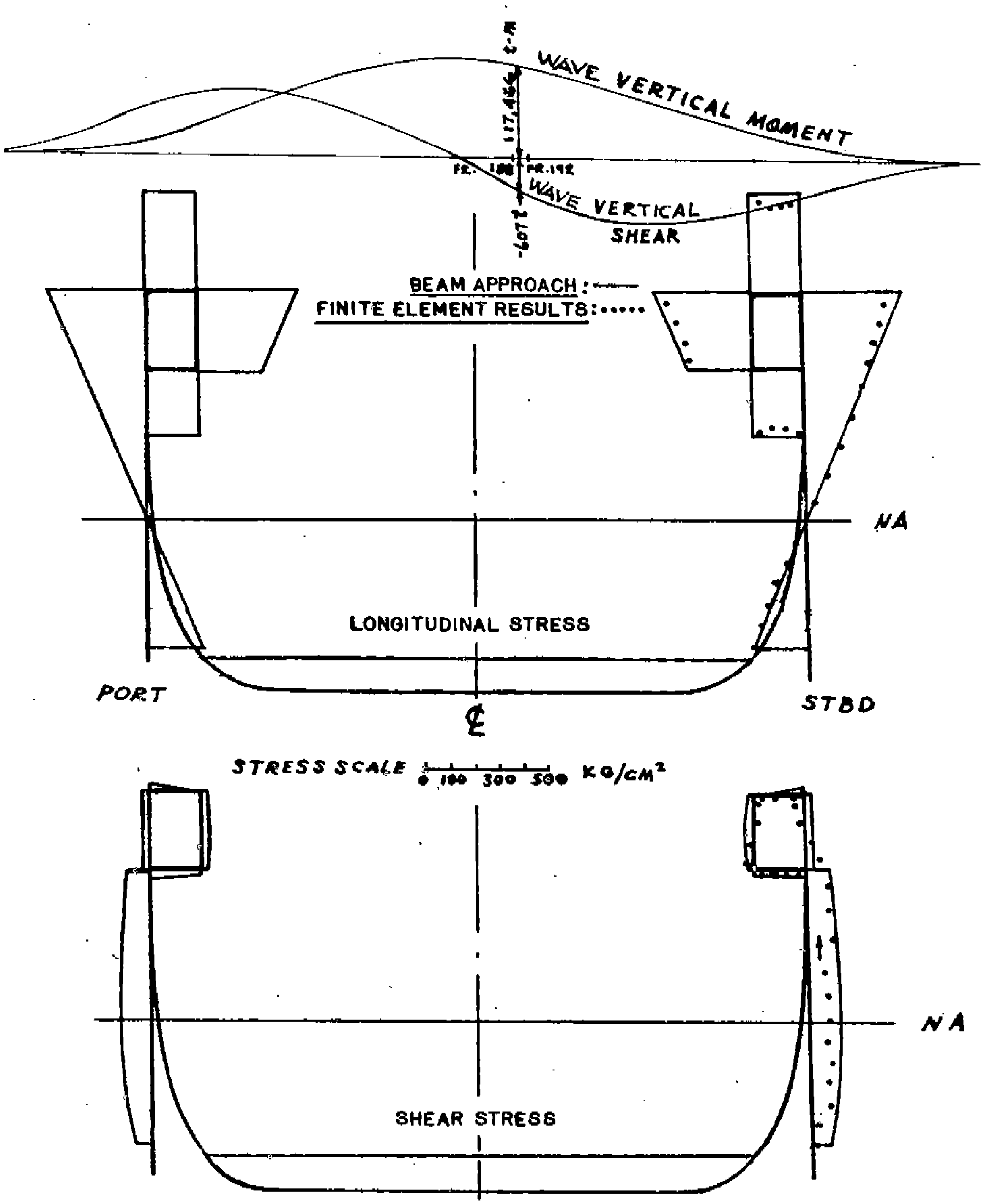

FIGURE 26 - STRESS DISTRIBUTIONS DUE TO WAVE INDUCED VERTICAL MOMENT AND SHEARING FORCES AT FR 190 - SECOND LOADING CASE

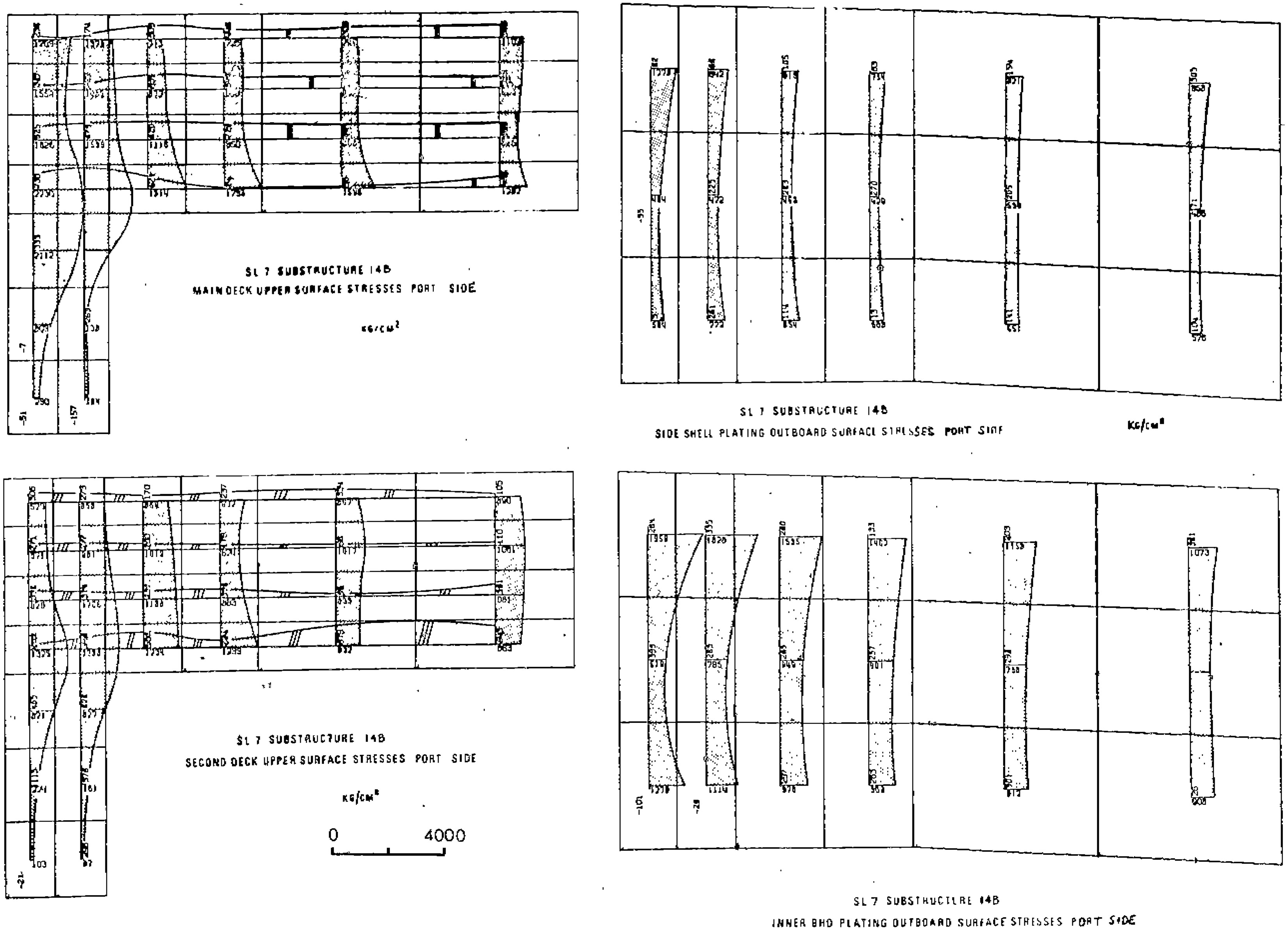

FIGURE 27 - LONGITUDINAL AND TRANSVERSE STRESSES - SUBSTRUCTURE FRS 142-150, PORT SIDE - FIRST LOADING CASE (REDUCED PLOTS)

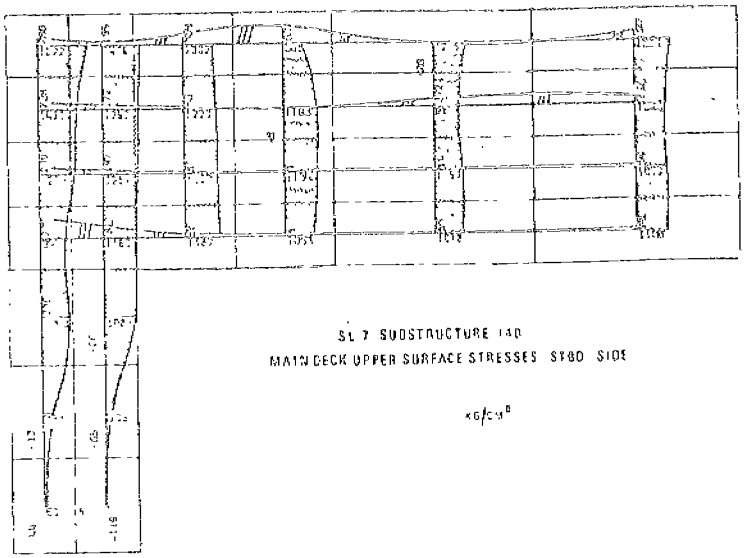

SL 7 SUBSTRUCTURE 14B
MAIN DECK UPPER SURFACE STRESSES STBD SIDE

KG/CM²

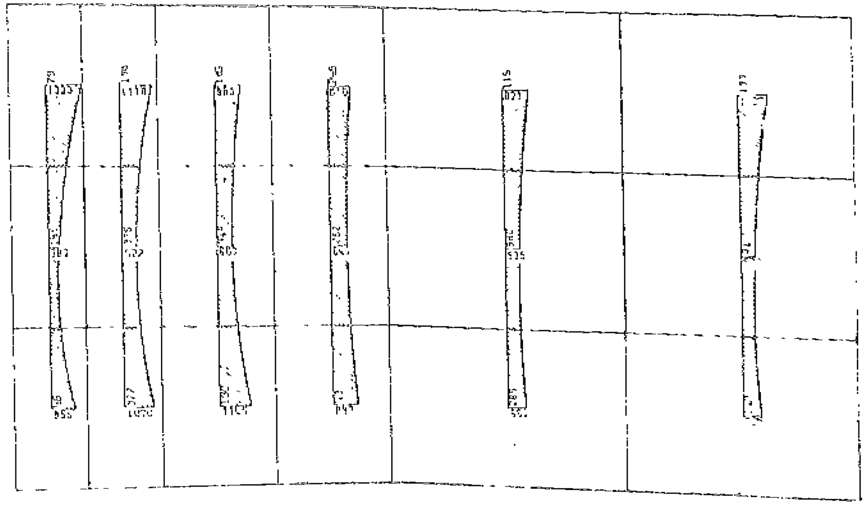

SL 7 SUBSTRUCTURE 14B
SIDE SHELL PLATING OUTBOARD SURFACE STRESSES STBD SIDE

KG/CM²

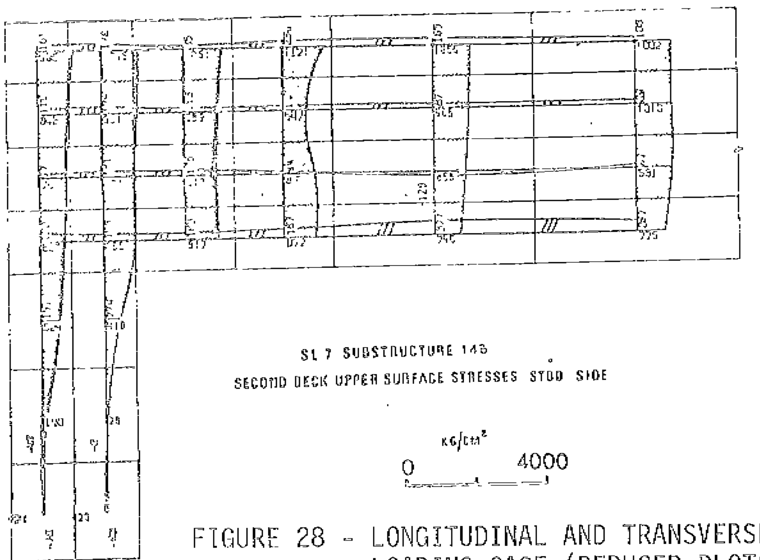

SL 7 SUBSTRUCTURE 14B
SECOND DECK UPPER SURFACE STRESSES STBD SIDE

KG/CM²
0 4000

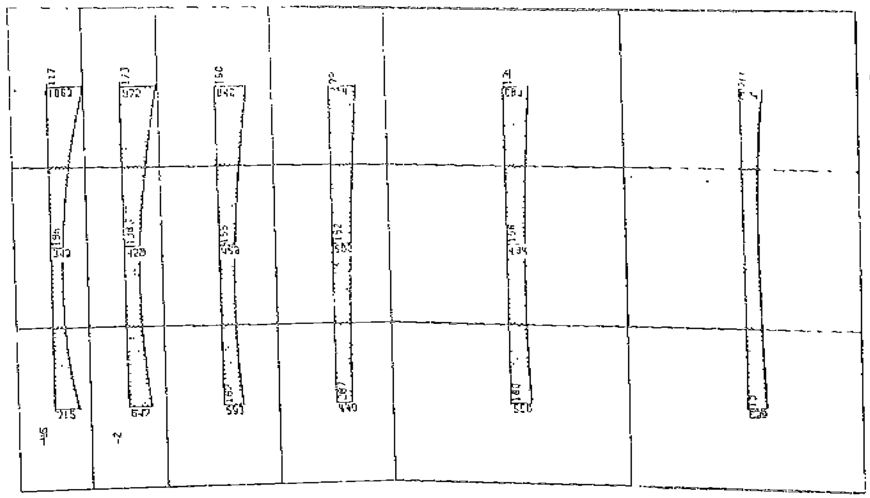

SL 7 SUBSTRUCTURE 14B
INNER BHD PLATING OUTBOARD SURFACE STRESSES STBD SIDE

KG/CM²

FIGURE 28 - LONGITUDINAL AND TRANSVERSE STRESSES - SUBSTRUCTURE FRS 142-150, STARBOARD SIDE - FIRST LOADING CASE (REDUCED PLOTS)

Figures 27 and 28 show the longitudinal stress distribution of substructure 14B, port and starboard sides. The restraint produced by the engine room housing is the cause of high stress magnitudes in the wing box, portside, in the deck area. The stresses on the inner bulkhead plating are higher than those of the shell plating; for the starboard wing box, the opposite is true. This is attributed to the effect of secondary lateral bending in the wing boxes. The results of the fine mesh model did not change this observation but it enabled us to detect the region of the highest shear stress near the hatch corner circular cutout. At frames 143-144 the stresses look almost uniform, Figure 29.

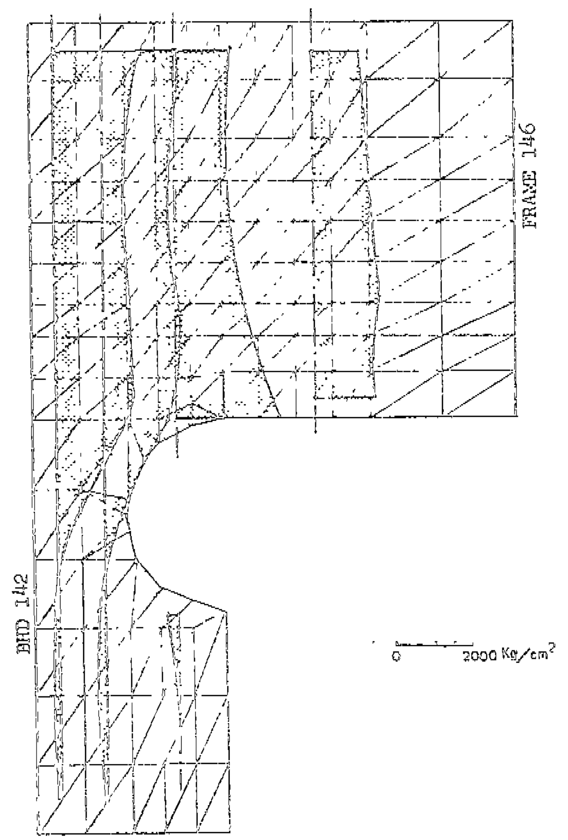

FIGURE 29 - MAIN DECK LONGITUDINAL STRESSES
FRS 142-146 PORT SIDE - MODEL 2 -
FINE MESH - FIRST LOADING CASE

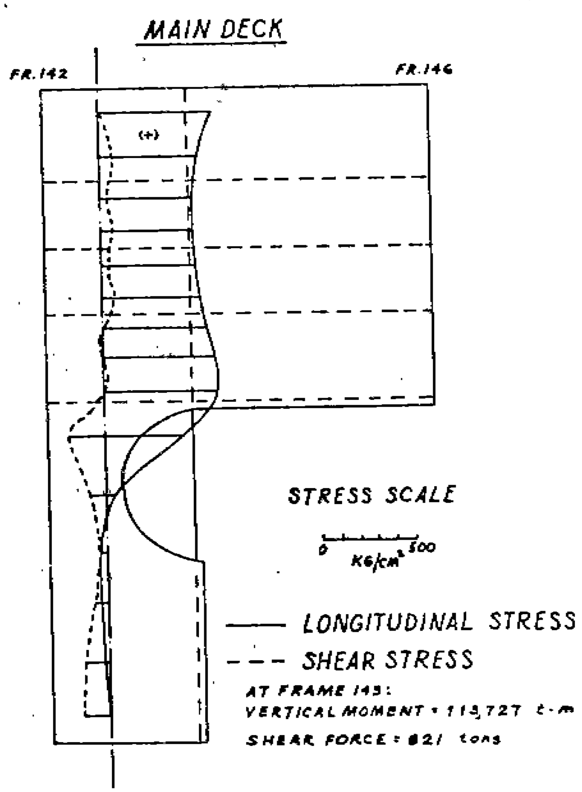

FIGURE 30 - STRESS DISTRIBUTION DUE TO WAVE INDUCED VERTICAL BENDING FR 142-146. SECOND LOADING CASE

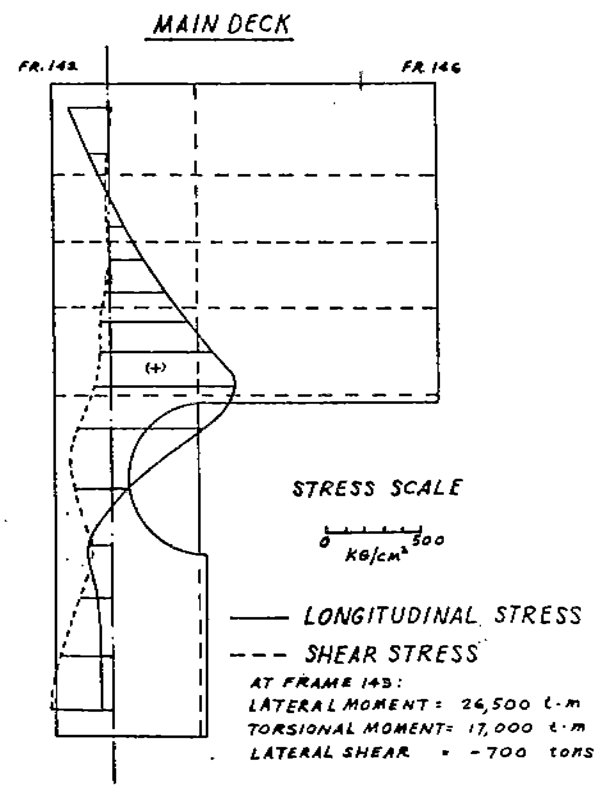

FIGURE 31 - STRESS DISTRIBUTION DUE TO LATERAL BENDING AND TORSIONAL MOMENTS, FR 142-146. SECOND LOADING CASE

The computed longitudinal and shear stress components in the main deck plating near Fr. 143 corresponding to the wave-induced vertical bending are shown in Figure 30. The stress components due to lateral bending and torsion are shown in Figure 31. It can be seen that the distribution of longitudinal stress components away from the hatch corner, due to pure wave-induced vertical bending, may be considered uniform, (Fig. 30), and those corresponding to lateral bending and torsion may be represented by a straight line (Fig.31).

<u>Wing Box-Transverse Box Connection at Frame 178.</u> Figures 32 through 40.

This portion of the deck structure is connected by two sub-structures, 9A and 9B, Figures 8, 10, and fine mesh model 1, Fig. 11.

Figures 33 and 34 show the longitudinal stress distribution of substructure 9A.

Figure 35 shows the fine mesh results of a part of the deck structure running between ship frames 176 and 182. The stress distribution on the deck is generally uniform at two locations, namely, frames 177 and 180-1/2. The longitudinal stress distribution around the wing box cross section is plotted, Figure 36, and compared with the stress results of substructure 9B at the same location. The stress pattern is as predicted in Figure 17.

Figure 37 shows the stress distribution around two sections of the transverse box. The transverse stresses obtained are the resultant of the two following components as illustrated in Fig. 32.

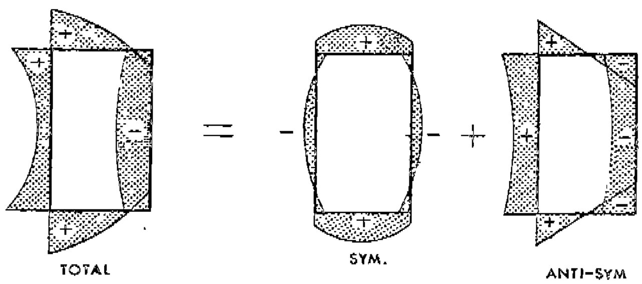

FIGURE 32 - STRESS RESOLUTION OF TRANSVERSE BOX, FR 178

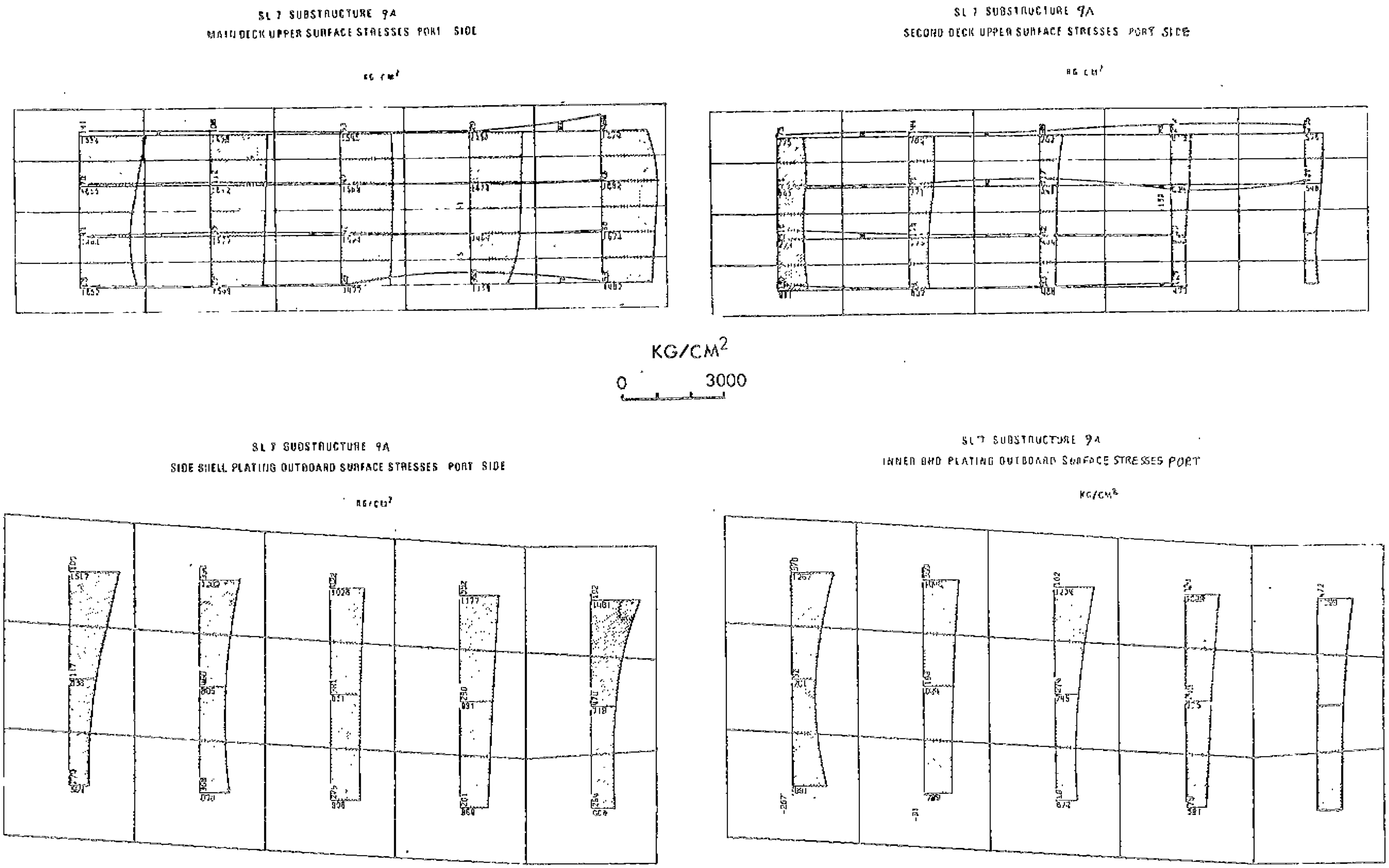

FIGURE 33 - LONGITUDINAL AND TRANSVERSE STRESSES - SUBSTRUCTURE FRS 168-178. PORT SIDE - FIRST LOADING CASE- (REDUCED PLOTS)

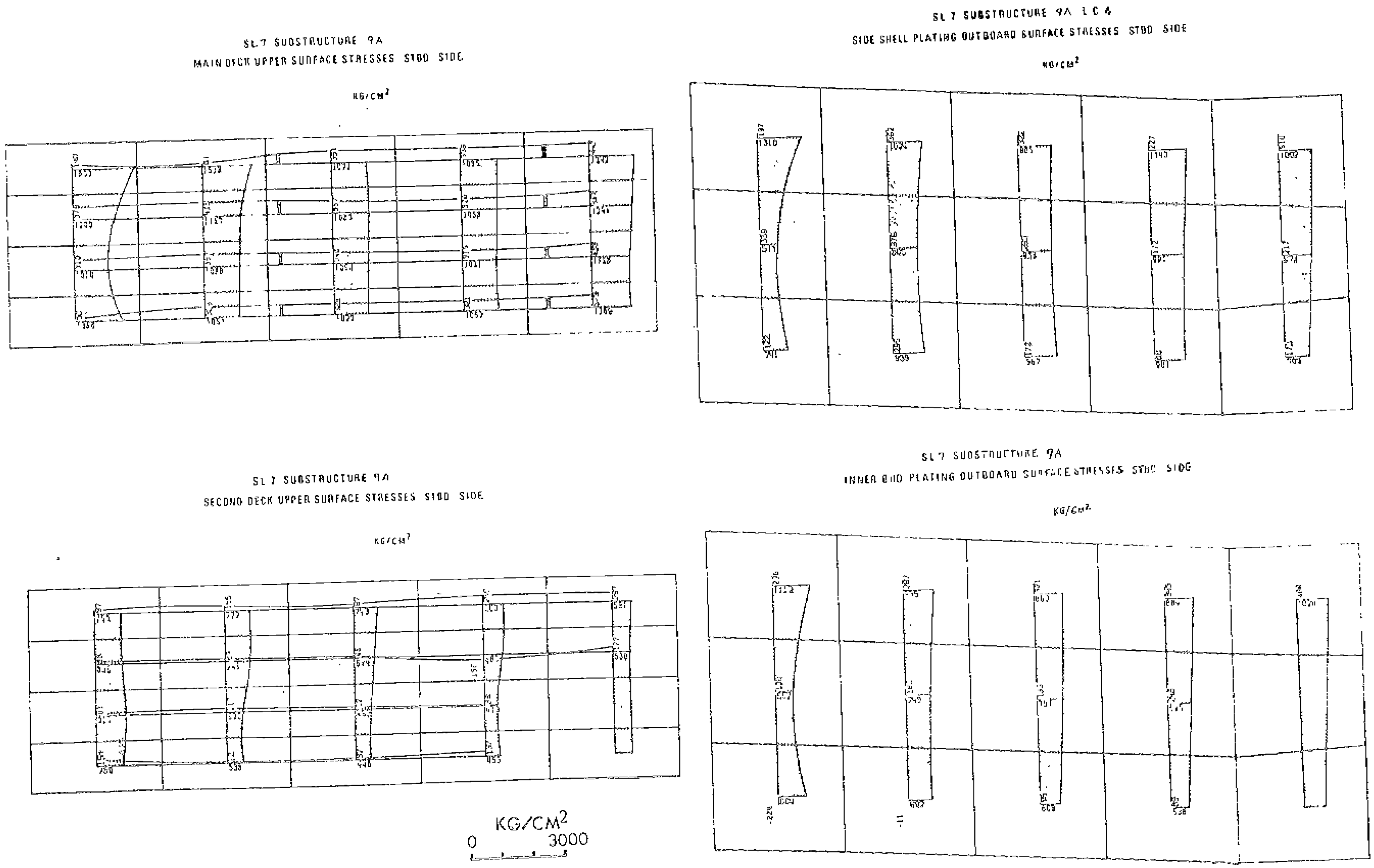

FIGURE 34 - LONGITUDINAL AND TRANSVERSE STRESSES - SUBSTRUCTURE FRS 168-178. STARBOARD SIDE - FIRST LOADING CASE - (REDUCED PLOTS)

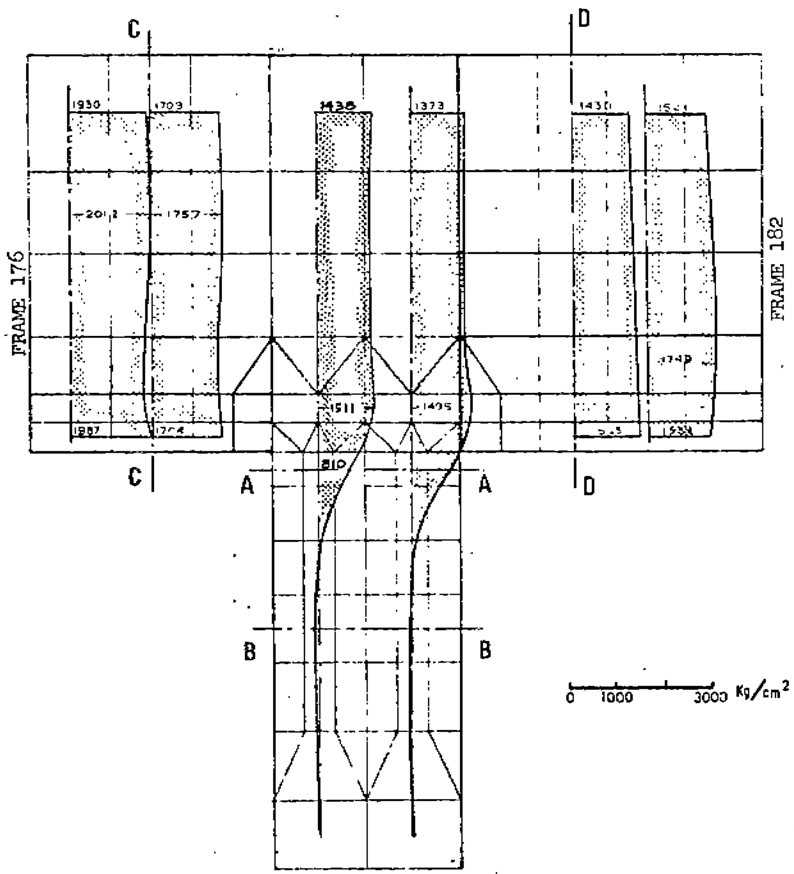

FIGURE 35 - MAIN DECK LONGITUDINAL STRESSES FRS 176-182 PORT SIDE - MODEL 1 FINE MESH - FIRST LOADING CASE

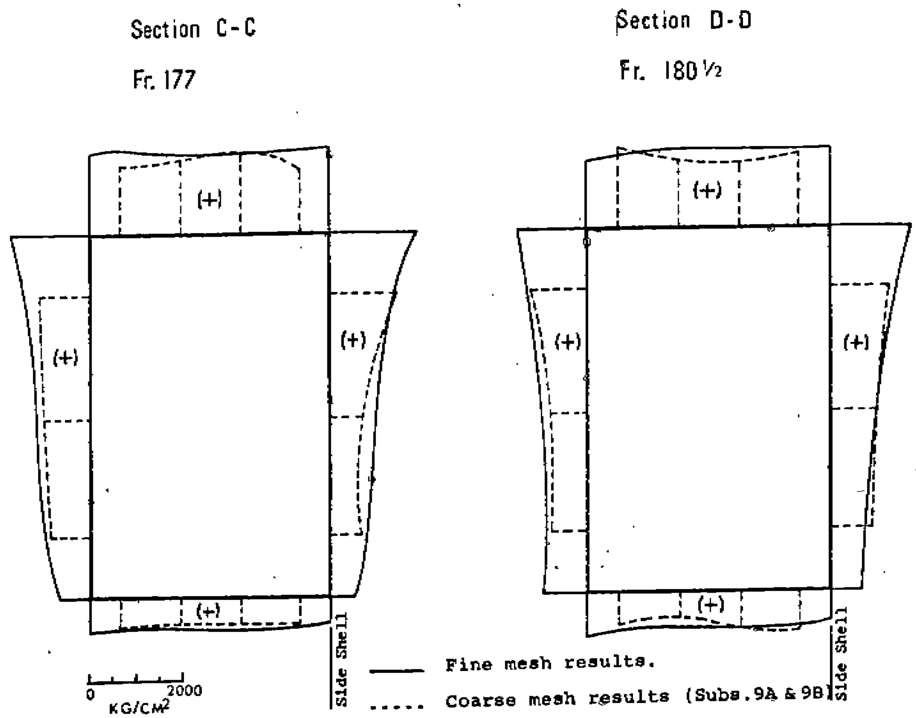

FIGURE 36 - LONGITUDINAL STRESSES - SUBSTRUCTURE MESH vs. FINE MESH RESULTS, PORT SIDE - FIRST LOADING CASE

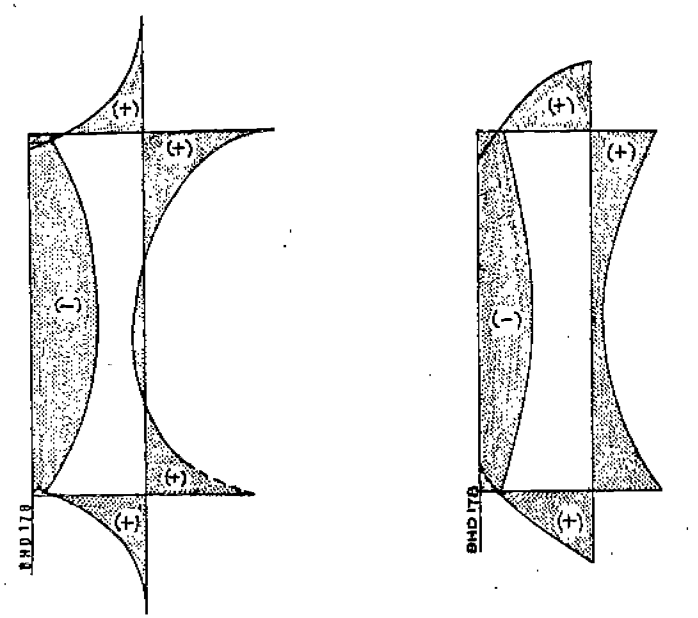

FIGURE 37 - TRANSVERSE BOX AT FR 178, PORT SIDE
FIRST LOADING CASE

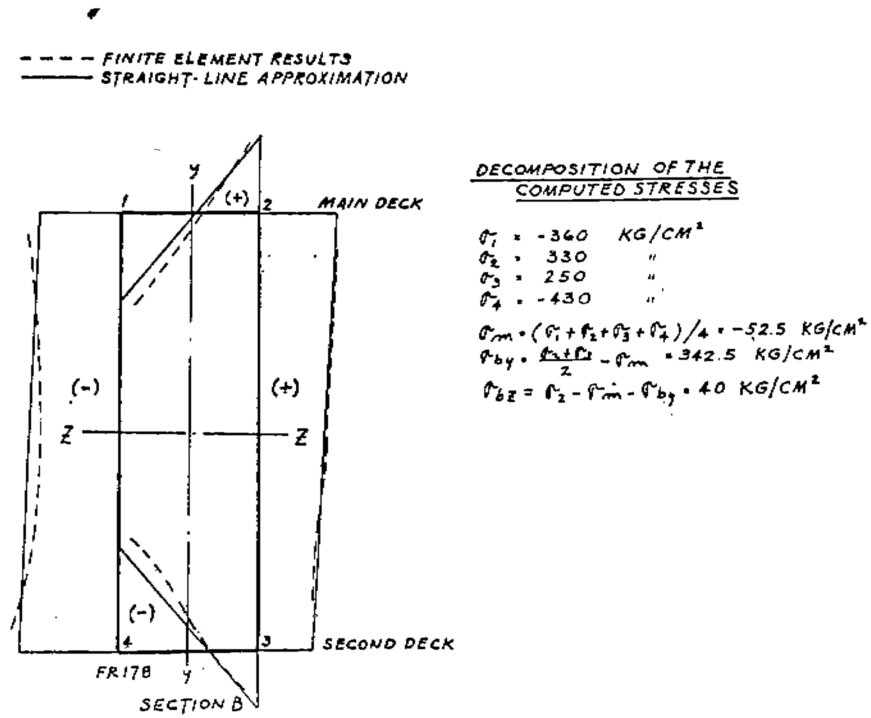

FIGURE 38 - ANTISYMMETRIC STRESSES ALONG TRANSVERSE BOX
AT FR. 178 - SECTION B PORT SIDE - FIRST
LOADING CASE

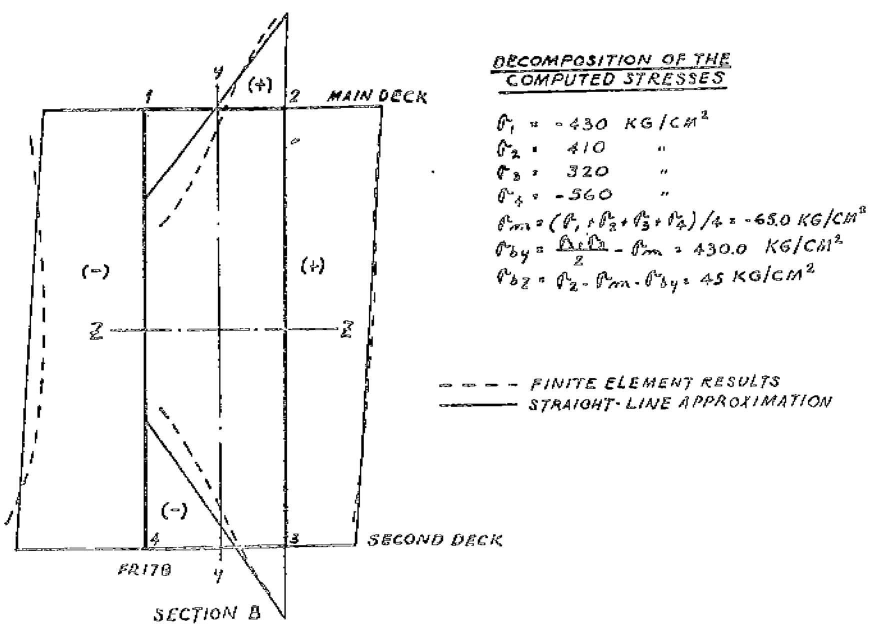

FIGURE 39 - ANTISYMMETRIC STRESSES ALONG TRANSVERSE BOX AT FR. 178, SECTION B PORT SIDE - SECOND LOADING CASE

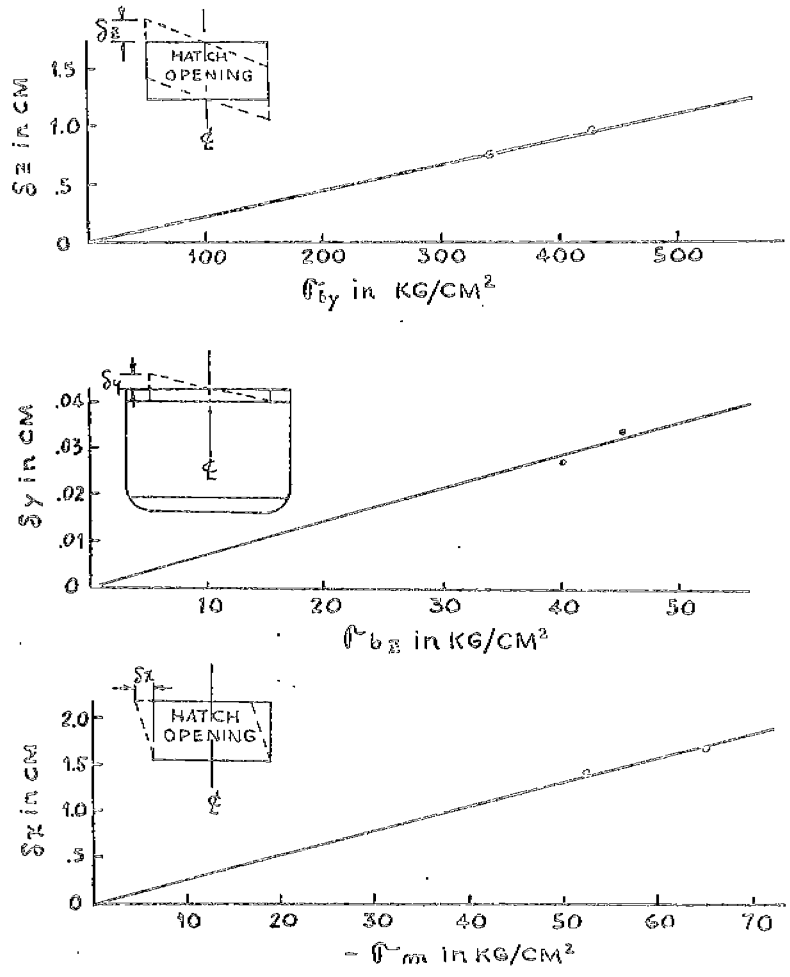

FIGURE 40 - HATCH DISTORTION vs. STRESSES IN TRANSVERSE BOX AT FR. 178, PORT SIDE - SECTION B DUE TO TORSIONAL AND LATERAL MOMENTS

The symmetric response is believed to be due to shear forces induced in the transverse box due to vertical bending of the ship.

The computed transverse stresses in the transverse box at Section B, Fig. 35, (corresponding to anti-symmetric loadings), are plotted in Figs. 38 and 39. In order to decompose the stresses into uniform axial and bending stress components, the distribution of the computed values is approximated by a straight line. The decomposition process is illustrated in those figures. The relationships between those stress components and the corresponding distortions of the hatch corner, obtained from the whole ship analysis are shown in Figure 40.

It should be noted that pure vertical bending also causes small distortion of hatch openings due to shear lag and secondary bending.

For a maximum vertical bending moment of 350,000 t-m, (1,148,000 ton. ft.) the distortion of hatch opening near midship is found to be δ_z = 0.25 cm, (0.10 inch) δ_y =0.126 cm, (0.05 inch). For the definition of δ_z and δ_y, see Figure 40.

STRESS DISTRIBUTION IN CONNECTION WITH STRAIN GAUGE INSTRUMENTATION.

The following are comments on the results obtained for the first loading case in the areas where strain gauges are installed on the "Sea-Land McLean" container ship.

At frame 143, the longitudinal stresses in the main deck of the wing box are generally uniform, and the proposed two strain gauge rosettes are adequate to obtain the mean stress value. Shear stresses are expected to be small in this area. At the hatch corner, the third rosette is expected to pick up a relatively high shear stress value yet small longitudinal stresses, Figures 30, 31.

At frame 226, similar sets of strain gauge rosettes are installed with the exception of two more rosettes at the hatch corner of the adjacent hatch. The computed stresses in this area show a similar pattern to those at frame 143. The stress magnitudes however, are much less, Figures 41, 42.

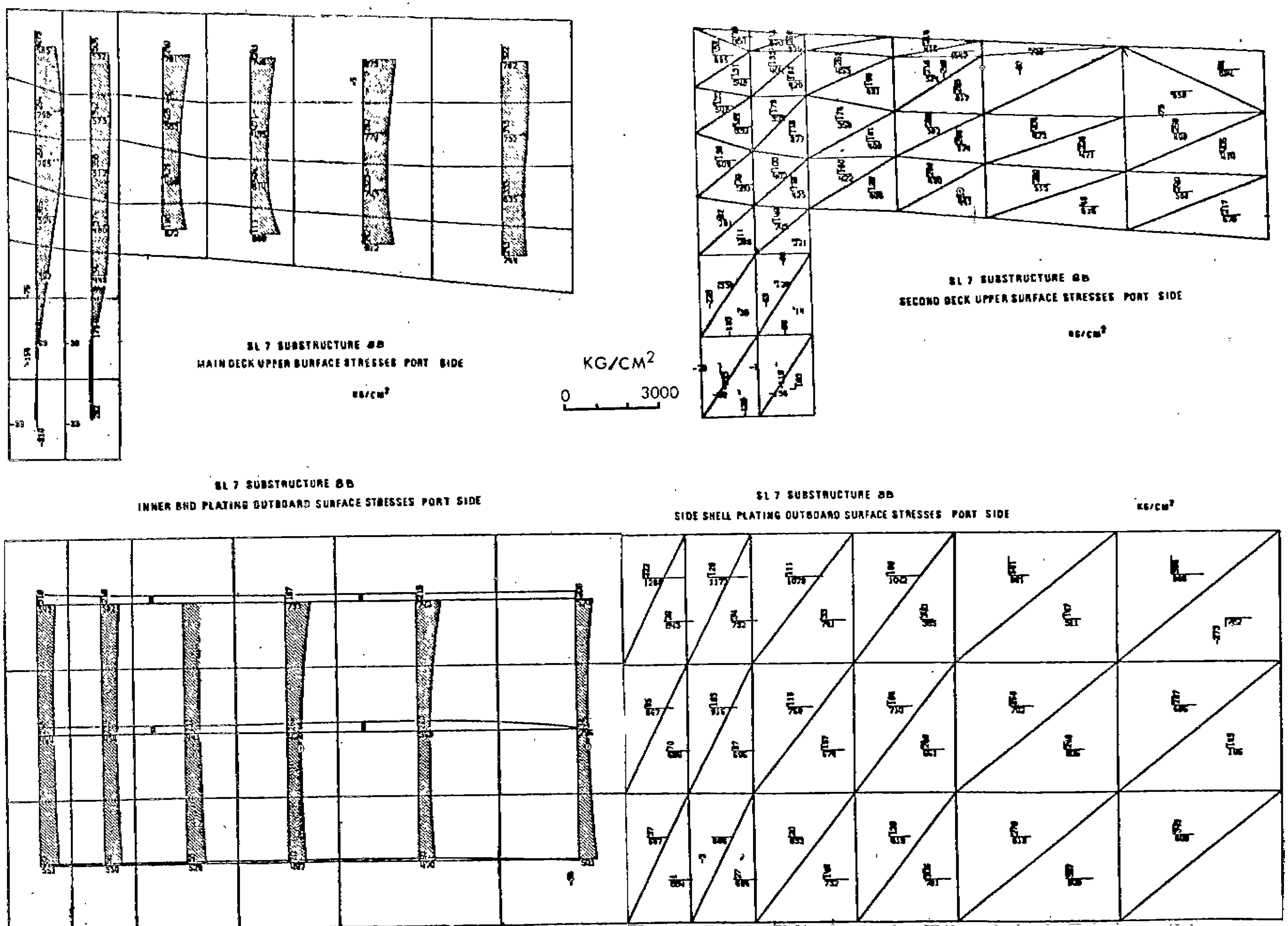

FIGURE 41 - LONGITUDINAL AND TRANSVERSE STRESSES - SUBSTRUCTURE FRS 226-235 PORT SIDE - FIRST LOADING CASE (REDUCED PLOTS)

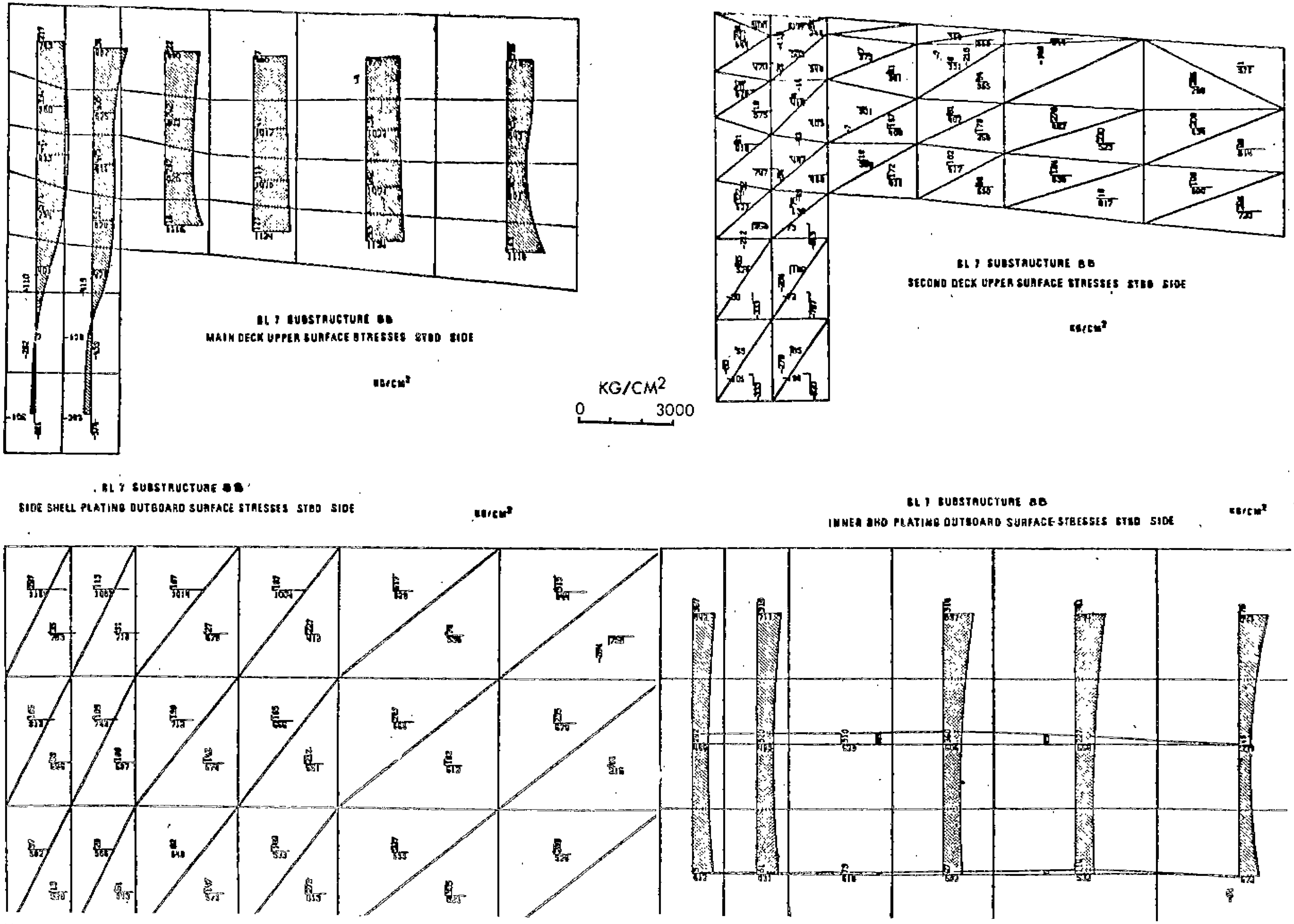

FIGURE 42 - LONGITUDINAL AND TRANSVERSE STRESSES - SUBSTRUCTURE FRS. 226-235. STARBOARD SIDE - FIRST LOADING CASE (REDUCED PLOTS)

In connection with the proposed so called "stress" gages at Fr. 186 1/4, port and starboard, (Ref. 9), the peak-to-peak vertical and lateral bending stresses which are in the order of 1,400 Kg/cm^2 (20,000 psi) and 900 Kg/cm^2 (13,000 psi), respectively, might be expected if the vessel would experience severe seas during the instrumentation period. It is expected that no significant warping stress will be recorded at this section because it is so close to the zero-twist point of the vessel.

At frame 259, a very coarse grid is used in this area. However, from the coarse mesh results, Figures 43, 44, and due to similarity in structural configuration to that location at frame 226, it is expected that the stress pattern will be the same.

There is no detail grid employed in the transverse box location, frames 78-80, 194-196 and 242-244. Since the second hatch forward of the engine room experienced the maximum hatch diagonal distortion, a portion of the transverse box frames 178-180 is included in fine mesh, model 1. The results are discussed previously, Figures 36 through 40.

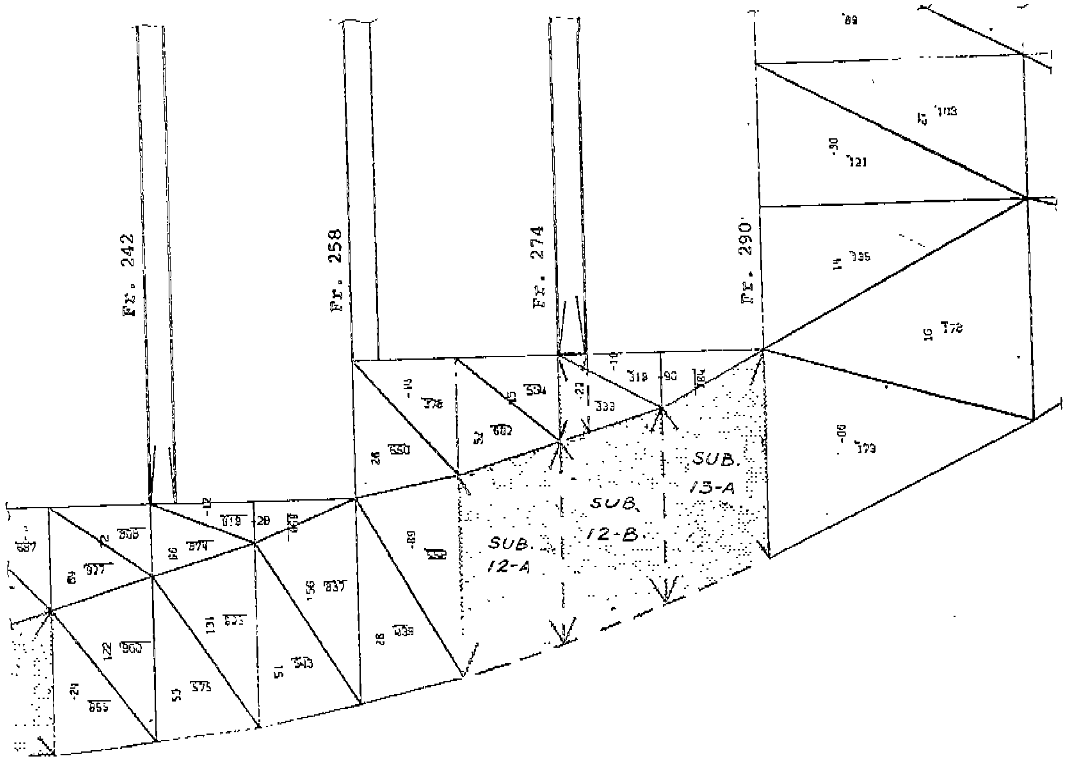

FIGURE 43 - COARSE MESH DECK STRESSES (KG/CM^2), STARBOARD SIDE, FIRST LOADING CASE

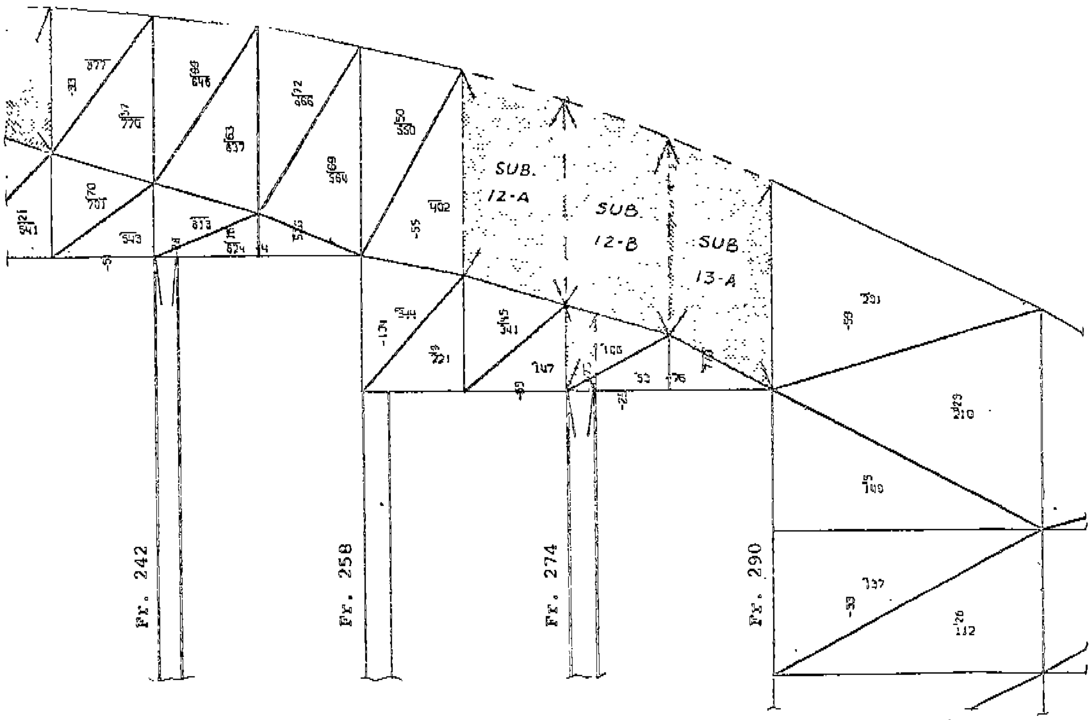

FIGURE 44 - COARSE MESH DECK STRESSES (KG/CM^2) PORT SIDE, FIRST LOADING CASE

Substructure 13-A, figures 45 through 47, is at the forward hatch between frames 282 and 290. Strain gages are installed at frame 290 mainly to measure the warping strain in this area. The rigid forward structure is believed to produce high torsional restraint. The maximum anti-symmetric stresses obtained near frame 290 are about 83 Kg/cm^2 (1180 psi) for the first loading case (port side) and about 94 Kg/cm^2 (1337 psi) for the second loading case.

The highest anti-symmetric stresses however, are obtained near frame 143 where the maximum value for the second loading case, port side, is about 650 Kg/cm^2 (9243 psi). These values include the lateral bending stress component and probably the local effects of the hatch corner. However away from the hatch corner, the anti-symmetric stress at frame 147 is about 300 Kg/cm^2 (4266 psi) and at frame 287 about 70 Kg/cm^2 (995 psi). Different torsional moment distributions may lead to different comparative stress figures.

Figures 46 through 48 show more stress results for substructure 9B, and substructure 8A near frame 225, where the deck opening is reduced.

It is worth noting that the substructuring of the deck locations was based on early proposed strain gage placement. However, in a later stage of the SL-7 instrumentation program and after the computer calculations were completed, more gages were assigned in locations not covered by substructures or fine mesh models. (Compare instrumentation plan (7) with substructure layout, Figure 8, and fine mesh models, Figure 11).

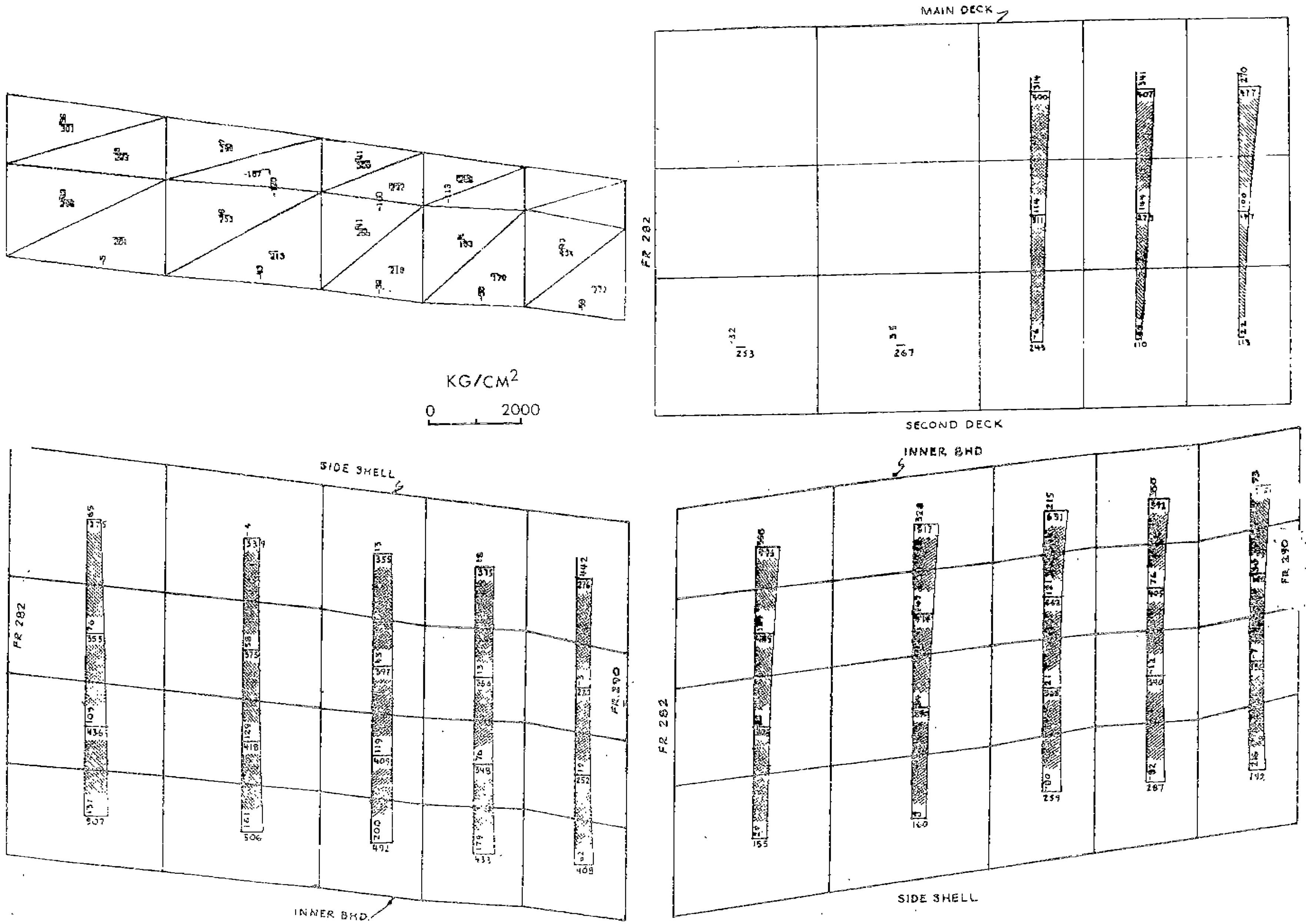

FIGURE 45 - LONGITUDINAL AND TRANSVERSE STRESSES - SUBSTRUCTURE FRS 282-290, PORT SIDE - FIRST LOADING CASE (REDUCED PLOTS)

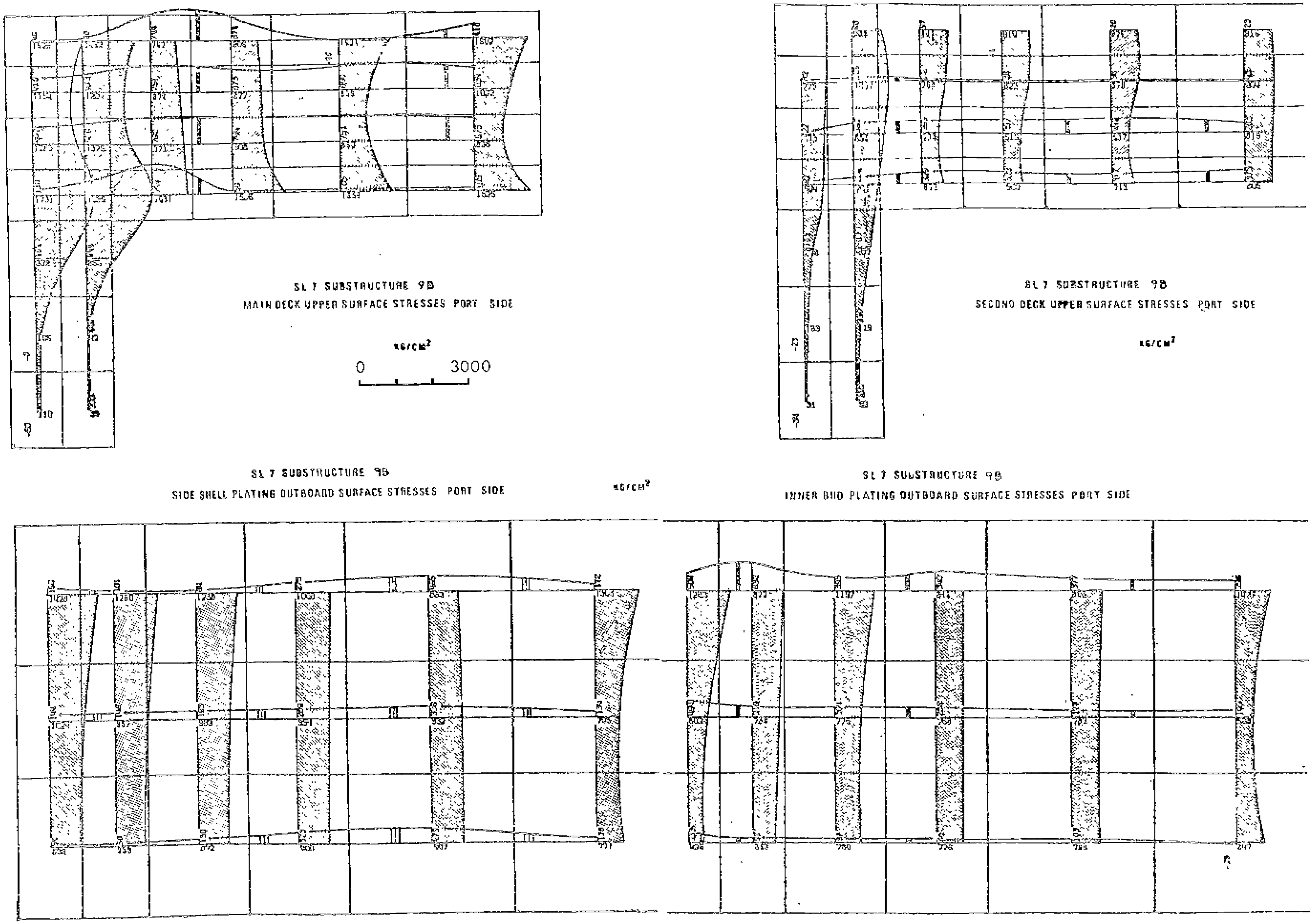

FIGURE 46 - LONGITUDINAL AND TRANSVERSE STRESSES - SUBSTRUCTURE FRS 178-187, PORT SIDE - FIRST LOADING CASE (REDUCED PLOTS)

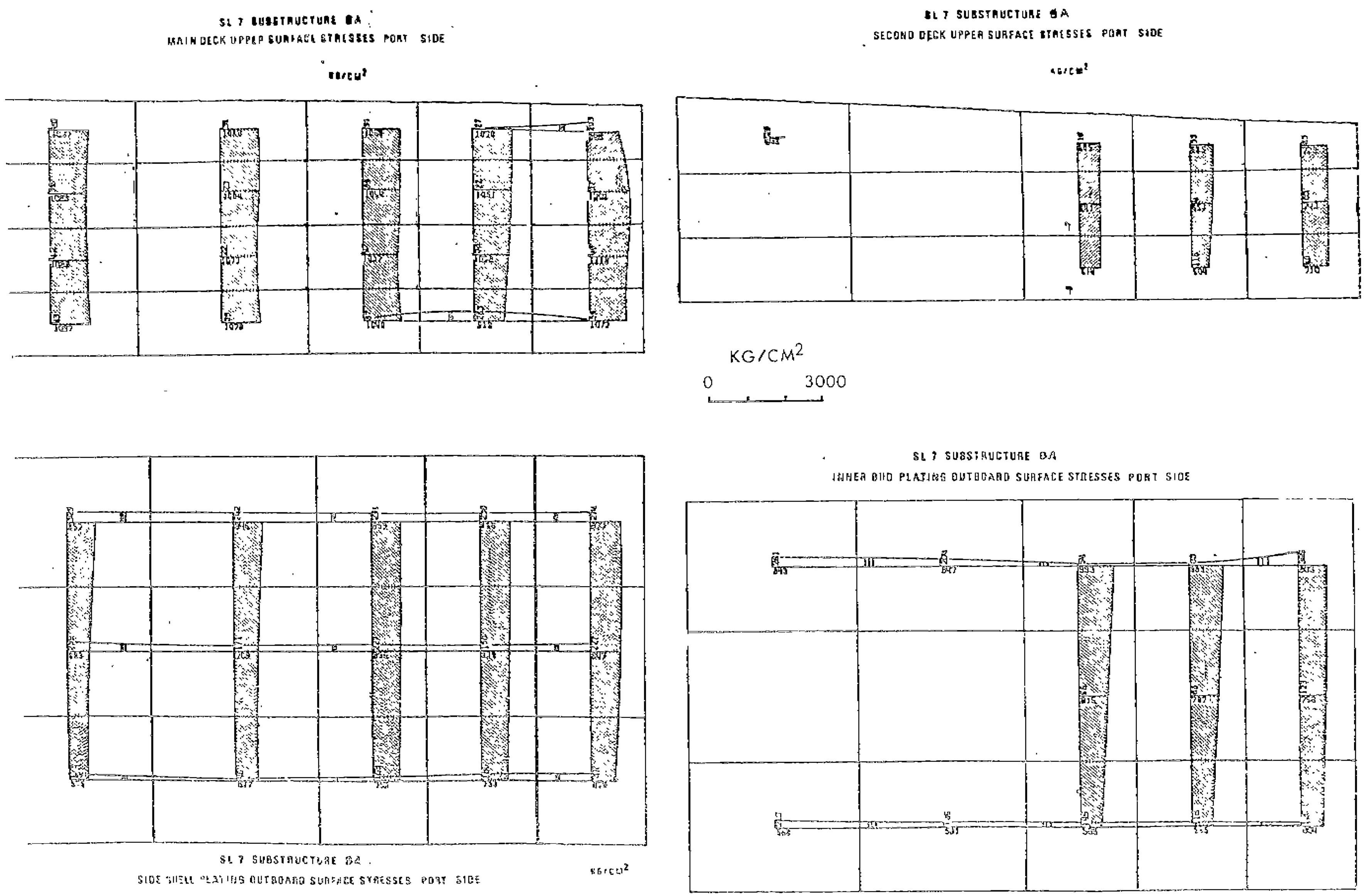

FIGURE 47 - LONGITUDINAL AND TRANSVERSE STRESSES - SUBSTRUCTURE FRS 218-226, PORT SIDE - FIRST LOADING CASE (REDUCED PLOTS)

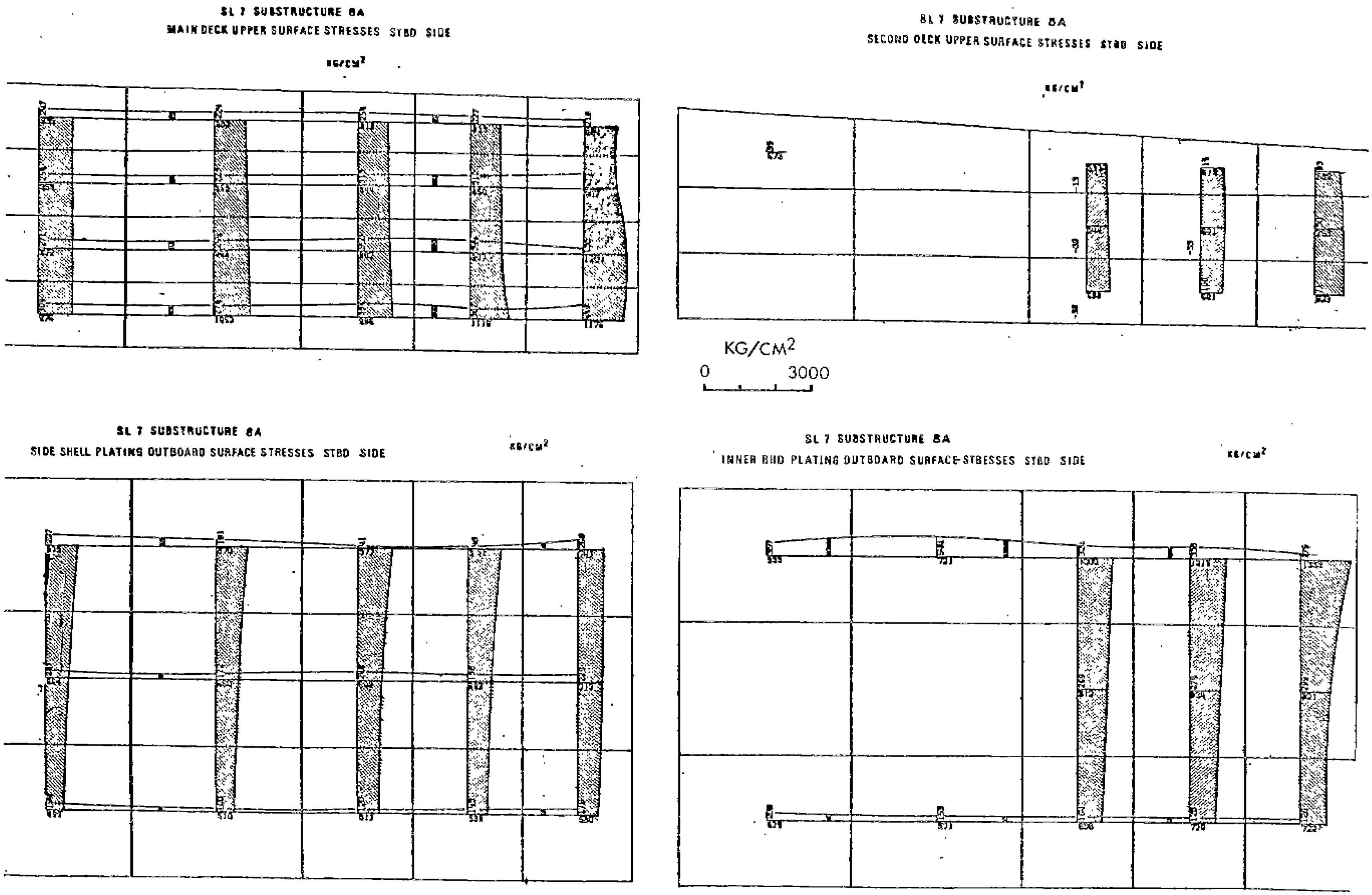

FIGURE 48 - LONGITUDINAL AND TRANSVERSE STRESSES - SUBSTRUCTURE FRS 218-226, STARBOARD SIDE - FIRST LOADING CASE (REDUCED PLOTS)

CHAPTER IV

CONCLUSIONS AND COMMENTS

1. Local deformation due to the non-prismatic nature of the structure and the deck openings can cause considerable increase in the total stress level as observed in the inner bulkhead plating of substructure 14-B, Figure 27.

2. A relationship between hatch distortion and the transverse box stress values is introduced. The finite element stress distribution in this area suggested the linearity of the stress pattern. This approach is to be verified by the experimental results when available.

3. The Navier Beam Hypothesis as applied to the open deck box girder appears to be adequate in predicting the primary response of the container ship under vertical bending moments.

4. Interpretations of the stress results at the locations of some strain gages on the "Sea-Land McLean" are made. Early output of the finite element results had helped in the determination of the final location of some gages.

5. For the first loading case, the following noteworthy values have been observed from the finite element calculations:

   a. Zero twisting angle is found near midship frame 190.

   b. The maximum diagonal hatch distortion amounted to 2.4 cms. (0.94 inch), in the second hatch forward of the engine room compartment.

   c. In deck areas where substructures were not employed, the maximum longitudinal stresses attained are about 1400 Kg/cm^2 (19,900 psi) on the port side and about 1300 Kg/cm^2 (18,486 psi) on the starboard side.

   d. On the side shell platings the maximum longitudinal stresses obtained are in the neighborhood of 2000 Kg/cm^2 (28,440 psi) between frames 210 and 242.

   e. A particular region of high stresses is found in the main deck forward of the engine room housing, frames 142-144. The maximum longitudinal stress at frame 143 is 2750 Kg/cm^2 (39,105 psi).

REFERENCES

1. Stiansen, S. G., Elbatouti, A., "Finite Element Analysis of Container Ships", Symposium on the Computer in Finite Element Analysis of Ship Structures, Tucson, Arizona, March, 1972.

2. O. Grim, "SL-7 Containership. Calculations of the Vertical, Horizontal and Torsional Loads Occurring in Waves", 1970, for J. J. Henry Co., Inc.

3. H. A. Kamel, et al. "The Computer in Ship Structure Design", ONR International Symposium on Numerical and Computer Methods in Structural Mechanics. The University of Illinois, September 1971, Urbana.

4. H. A. Kamel, A. Elbatouti, "DAISY Engineers Manual", Volumes 1, 2, August 1970, American Bureau of Shipping, University of Arizona.

5. H. A. Kamel, A. Miller, "DAISY, Programmers' Manual", May 1972, American Bureau of Shipping, University of Arizona.

6. D. Liu, "SHIPMOM", "EXAM", "EXPLOT", "LOADER", Engineering Manuals, August 1970, American Bureau of Shipping, University of Arizona.

7. Design and Installation of a Ship Response Instrumentation System Aboard the SL-7 Class S.S. Sea-Land McLean. Teledyne Materials Research, E-1395 (b).

ACKNOWLEDGEMENT

The authors are indebted to Sea Land Services, Inc. for providing all the information on the ship subject to the analysis.

The authors also wish to acknowledge the efforts of Dr. Hussein Kamel, Professor, Aerospace and Mechanical Engineering Department, University of Arizona, who is the author of the DAISY computer program.

Appreciation is also extended to many members of the Research and Development Department of the American Bureau of Shipping for their efforts and assistance.

Security Classification

DOCUMENT CONTROL DATA - R & D

(Security classification of title, body of abstract and indexing annotation must be entered when the overall report is classified)

1. ORIGINATING ACTIVITY (Corporate author) American Bureau of Shipping	2a. REPORT SECURITY CLASSIFICATION Unclassified 2b. GROUP

3. REPORT TITLE

STRUCTURAL ANALYSIS OF SL-7 CONTAINERSHIP UNDER COMBINED LOADING OF VERTICAL, LATERAL & TORSIONAL MOMENTS USING FINITE ELEMENT TECHNIQUES

4. DESCRIPTIVE NOTES (Type of report and inclusive dates)

5. AUTHOR(S) (First name, middle initial, last name)

A. M. Elbatouti, D. Liu, and H. Y. Jan

6. REPORT DATE	7a. TOTAL NO. OF PAGES	7b. NO OF REFS
May 1974	48	7

8a. CONTRACT OR GRANT NO.	9a. ORIGINATOR'S REPORT NUMBER(S)
b. PROJECT NO.	SSC-243
c.	9b. OTHER REPORT NO(S) (Any other numbers that may be assigned this report) SL-7-3
d.	

10. DISTRIBUTION STATEMENT

Distribution of this document is unlimited

11. SUPPLEMENTARY NOTES	12. SPONSORING MILITARY ACTIVITY
	Naval Ship Systems Command

13. ABSTRACT

The entire SL-7 container vessel hull structure is analyzed by the DAISY finite element computer program. The ship, loaded with containers, placed in oblique quasi-static regular waves, is subject to combined vertical, lateral and torsional loads. Stress distributions particularly in the deck region are presented and investigated from the analysis using the reduced element substructure feature in the program. Fine mesh analyses are also presented at different locations of the ship. The computed stresses are discussed in connection with the placement of strain gages instrumentation on the "SEA-LAND McLEAN".

DD FORM 1 NOV 65 1473 (PAGE 1)

S/N 0101-807-6801

Security Classification

14 KEY WORDS	LINK A		LINK B		LINK C	
	ROLE	WT	ROLE	WT	ROLE	WT

SHIP RESEARCH COMMITTEE
Maritime Transportation Research Board
National Academy of Sciences-National Research Council

The Ship Research Committee has technical cognizance of the interagency Ship Structure Committee's research program:

PROF. J. E. GOLDBERG, Chairman, *School of Civil Engineering, Purdue University*
PROF. R. W. CLOUGH, *Prof. of Civil Engineering, University of California*
DR. S. R. HELLER, Jr., *C'man, Civil & Mech. Eng. Dept., The Catholic Univ. of America*
MR. G. E. KAMPSCHAEFER, Jr., *Manager, Technical Services, ARMCO Steel Corporation*
MR. W. W. OFFNER, *Consulting Engineer, San Francisco*
MR. D. P. ROSEMAN, *Chief Naval Architect, Hydronautics, Inc.*
MR. R. C. STRASSER, *Director of Research, Newport News Shipbuilding & Dry Dock Co.*
MR. H. S. TOWNSEND, *Vice President, U.S. Salvage Association, Inc.*
DR. S. YUKAWA, *Consulting Engineer, General Electric Company*
MR. R. W. RUMKE, *Executive Secretary, Ship Research Committee*

Advisory Group I, "Ship Response and Load Criteria", prepared the project prospectus and evaluated the proposals for this project:

MR. D. P. ROSEMAN, Chairman, *Chief Naval Architect, Hydronautics, Inc.*
PROF. J. L. BOGDANOFF, *School of Aeronautics & Astronautics, Purdue University*
MR. M. D. BURKHART, *Head, Marine Science Affairs, Office of Oceanographer of the Navy*
DR. C. CHRYSSOSTOMIDIS, *Asst. Prof. of Naval Architecture, Mass. Inst. of Technology*
MR. C. W. COWARD, *Hull Technical Manager, Newport News Shipbuilding & Dry Dock Co.*
DR. R. GLASFELD, *Naval Architect, General Dynamics Corporation*
DR. J. E. HALKYARD, *Senior Ocean Engineer, Kennecott Exploration, Inc.*
DR. N. H. JASPER, *Technical Director, Naval Coastal Systems Laboratory*
MR. R. G. KLINE, *Assoc. Research Consultant, U.S. Steel Corporation*
PROF. J. LANDWEBER, *Institute of Hydraulic Research, The University of Iowa*
DR. M. K. OCHI, *Research Scientist, Naval Ship Research & Development Center*
PROF. J. C. SAMUELS, *Dept. of Electrical Engineering, Howard University*
PROF. M. SHINOZUKA, *Dept. of Civil Engineering & Eng. Mechanics, Columbia University*
PROF. R. A. YAGLE, *Prof. of Naval Architecture, University of Michigan*

The SL-7 Program Advisory Committee provided the liaison technical guidance, and reviewed the project reports with the investigator:

MR. R. C. STRASSER, Chairman, *Dir. of Research, Newport News Shipbuilding & Dry Dock Co.*
MR. E. R. ASHEY, *Asst. for Advanced Technology, Naval Ship Engineering Center*
PROF. E. V. LEWIS, *Director of Research, Webb Institute of Naval Architecture*
MR. J. H. ROBINSON, *Staff Naval Architect, Naval Ship Research & Development Center*
MR. D. P. ROSEMAN, *Chief Naval Architect, Hydronautics, Inc.*
PROF. R. A. YAGLE, *Prof. of Naval Architecture, University of Michigan*

SHIP STRUCTURE COMMITTEE PUBLICATIONS

These documents are distributed by the National Technical Information Service, Springfield, Va. 22151. These documents have been announced in the Clearinghouse journal U.S. Government Research & Development Reports (USGRDR) under the indicated AD numbers.

SSC-234, *Evaluation of Methods for Extrapolation of Ship Bending Stress Data* by D. Hoffman, R. van Hooff, and E. V. Lewis. 1972. AD 753224

SSC-235, *Effect of Temperature and Strain Upon Ship Steels* by R. L. Rothman and R. E. Monroe. 1973. AD 768891

SSC-236, *A Method for Digitizing, Preparing and Using Library Tapes of Ship Stress and Environment Data* by A. E. Johnson, Jr., J. A. Flaherty, and I. J. Walters. 1973. AD 767388

SSC-237, *Computer Programs for the Digitizing and Using of Library Tapes of Ship Stress and Environment Data* by A. E. Johnson, Jr., J. A. Flaherty, and I. J. Walters. 1973. AD 768863

SSC-238, *Design and Installation of a Ship Response Instrumentation System Aboard the SL-7 Class Containership S.S. SEA-LAND McLEAN* by R. A. Fain. 1974.

SSC-239, *Wave Loads in a Model of the SL-7 Containership Running at Oblique Headings in Regular Waves* by J. F. Dalzell and M. J. Chiocco. 1974.

SSC-240, *Load Criteria for Ship Structural Design* by E. V. Lewis, R. van Hooff, D. Hoffman, R. B. Zubaly, and W. M. Maclean. 1973. AD 767389.

SSC-241, *Thermoelastic Model Studies of Cryogenic Tanker Structures* by H. Becker and A. Colao. 1973. AD 771217

SSC-242, *Fast Fracture Resistance and Crack Arrest in Structural Steels* by G. T. Hahn, R. G. Hoagland, M. F. Kanninen, A. R. Rosenfield and R. Sejnoha. 1973. AD 775018

SL-7 PUBLICATIONS TO DATE

SL-7-1, (SSC-238) - *Design and Installation of a Ship Response Instrumentation System Aboard the SL-7 Class Containership S.S. SEA-LAND McLEAN* by R. A. Fain. 1974.

SL-7-2, (SSC-239) - *Wave Loads in a Model of the SL-7 Containership Running at Oblique Headings in Regular Waves* by J. F. Dalzell and M. J. Chiocco. 1974.

SL-7-3, (SSC-243) - *Structural Analysis of SL-7 Containership Under Combined Loading of Vertical, Lateral and Torsional Moments Using Finite Element Techniques* by A. M. Elbatouti, D. Liu and H. Y. Jan. 1974.